Investigation of Corona Discharges and Electrical Breakdown in Sulphur-hexafluoride/Nitrogen Mixtures

by

Wong Ka Ming

(9698)

Thesis Report

Submitted in partial satisfaction of the requirements for the degree of

Master of Philosophy

in

Electrical Engineering

of

The Hong Kong Polytechnic University

January 2002

Abstract

These days, corona was studied and investigated in different mixture ratio of SF_6 and N_2 by observing the pulse shape and frequency and the average current for a range of voltages from onset to breakdown. Models for the corona behaviour were developed and simulation programs written based on various proposed models for the ionisation and attachment parameters of gas mixtures. An important aspect was the use of the symmetrical point/cup electrode system introduced by MacAlpine, my supervisor whose symmetry allows the development of mathematical models not possible with the more traditional point/plane electrode system. A thorough understanding of the pre-breakdown (corona) phenomena is likely to lead to an explanation for the breakdown strength. The measurements were carried out over a range of pressures up to the commercially and industrially important 5-bar level. Both voltage polarities were studied.

Experiments conducted in point-cup gaps can be considered to represent the geometric conditions in practical gas-insulated switchgear which are commonly used in power systems, where the breakdowns tend to originate with small metallic particles and the corona which develops at their pointed end. The mechanism of breakdown originating with a long metallic particle on the 'floor' of the earthed outer tube has some similarity with that of the point/plane system.

Table of Contents

Chapter 1

Introduction

Chapter 1 - Introduction

When a high voltage is applied across the electrodes with a gap in between, discharge or breakdown may occur depending on some parameters e.g. geometry of the electrodes. In uniform field gaps, the onset of measurable ionisation leads, with increasing voltage, to complete breakdown of the gap. In non-uniform fields, various manifestations of luminous and audible discharges are observed long before the complete breakdown occurs. These discharges may be transient or steady state and are known as "coronas" [1,3,4]. Corona [1] is described as a small electrical discharge from a small peak or ridge on the surface of a conductor. As the point has a much higher electric field than the smoother parts of the conductor, corona discharge always occurs at a relatively low voltage.

One of the electrode configurations that leads itself quite satisfactorily for experimental and theoretical studies of corona is the sphere with a radius chosen according to the degree of field nonuniformity desired [2]. Due to the symmetrical electric field across the gap of point/cup system, the simulation algorithm is simplified to one dimension rather than the three dimensions of point/plane systems.

Sulphur hexafluoride (SF_6) is the most commonly used insulating gas in electrical systems. Gas-insulated systems are widely used in the electric power industry for transmission and distribution of electrical energy. It has good dielectric properties. The breakdown strength is nearly three times higher than that of air at atmospheric pressure.

However, in order to reduce the greenhouse effect (global warming) caused by SF_6, the release of SF_6 into the atmosphere must be avoided or at least carefully limited. For long-term solutions, SF_6 should be replaced by another gas with acceptable breakdown strength. Among the possible gas mixtures, SF_6/N_2 is considered as this mixture exhibits many of the desirable properties of SF_6 as a gaseous dielectric. Unlike SF_6, nitrogen (N_2) is the main component of air, and widely used in many technical and industrial applications. As a gas mixture with SF_6, nitrogen scatters energetic electrons into the low-energy region where the electronegative gas SF_6 captures them with highest efficiency and thereby inhibits the buildup of electrons that could produce ionisation leading to electrical breakdown [8].

In the present work, corona discharges in SF_6/N_2 mixtures are reported using the point/cup system with the long-term intention of understanding in order to study the mechanism of breakdown in non-uniform fields. Apart from the academic importance, there is the practical importance of understanding the breakdown of gas-insulated switchgear due to the presence of metallic particles on the 'floor' of the earthed outer tube. The effect of pressure and the diameter of the point electrode on the onset voltage with various mixture ratios have been observed and attention has been paid to the pre-breakdown characteristics. The experimental and simulated results will be analysed and compared with each other.

Chapter 2

Literature Survey and Background Theory

Chapter 2 - Literature Survey and Background Theory

2.1 Introduction

Research into corona discharges in SF_6/N_2 mixtures has been done for a few decades [1-48]. Many investigations have been reported in the literature on the breakdown behaviour of SF_6/N_2 mixture [1,4,6,8,10,14,17-19,28,31]. However, most of the published data refers to dc and ac voltages in uniform or nearly uniform field gaps [1,5-8,18,22,35,38,41,42,46,47]. As part of an extensive study of gaseous dielectric behaviour, we are investigating the mixtures in non-uniform field gaps. As the mixture proved to have many desirable properties to be a good dielectric as compared with pure SF_6, experiments were done to find out the characteristics of this mixture. Some measurements were made of corona pre-breakdown currents, usually with point/plane electrode systems, before the 1970's [4,17,20,21,23,25,29,32,36,37,40,45] and qualitative explanations for the observed phenomena were advanced. However, quantitative modelling and explanations have been lacking.

With accurate, reliable and faster computing systems recently, different models have been developed to simulate most forms of pre-breakdown phenomena in gases [4,5,15,20,21,35,46,48]. In the past decade, methods to predict the breakdown behaviour of SF_6/N_2 mixtures were very desirable. Methods of estimation of the minimum discharge voltage of the mixture were developed. In 1979, Malik and Qureshi [5,6] calculated the onset voltage from basic principles and compared it with the experimental measurements.

The results showed that the calculated values are in reasonably good agreement with experimental measurements for gaps having varying degrees of field non-uniformities and over a specified pressure range.

The calculations and simulations of discharge behaviour have been described in some papers. However they cannot predict the sudden disappearance of the streamer pulses just above the positive point onset voltage which is due to the build-up of space charge around the point electrode. Morrow [30], and Liu and Govinder Raju [15, 20, 21, 35] only considered ionisation activity along the gap axis, and only for the first pulse of a sequence. However the first pulse is different from subsequent 'space-charge' pulses because of the 'space-charge' remaining in the gap from the previous pulses.

On the other hand, many researchers suggested that the space charge field of the primary and subsequent electron avalanches should not be neglected in calculating corona onset voltages based on streamer criterion. At 1979, Parekh and Srivastava [7] wrote a program to simulate this space charge effect, due to both electrons and positive ions, on the onset voltage in air and SF_6, and the result indicated that the effect was to reduce the corona onset voltage by less than 5%, which is the opposite of what is found in practice. Furthermore, the space charge effect plays an important role in the breakdown and pre-breakdown characteristics of corona discharge [2,3]. No more recent attempts at simulation appear to have been developed to account for this effect because the corona and phenomena are not yet thoroughly understood.

The majority of those reported works are just experimental results with qualitative explanations. Part of the problem is due to the use of traditional point/plane electrode system which has a complex field pattern between the electrodes. Every flux line has a different field-distance relationship. So a point/cup electrode system was used in present studies, as its symmetry allows simplified analysis and simulation. So all flux-lines between the electrodes have same length and the same field distribution along them. A simulation program, derived by MacAlpine and Li recently [2,28], which took advantage of the spherical symmetry of a point/cup electrode system and assumed avalanches to originate from the random release of electrons in the inter-electrode gap, gave good general agreement with measured corona onset voltages in the absence of space charge effects and justified the approach.

In 1995, Christophorou and Van Brunt [8] wrote a lengthy paper reviewing all the available data and information relevant to the use of SF_6/N_2 gas mixtures as gaseous dielectrics in HV insulation. The physical and chemical properties of pure SF_6, pure N_2 and SF_6/N_2 mixture given in previous papers were included. The uniform and non-uniform field breakdown and corona characteristics of the mixtures were also discussed extensively.

To sum up, as the breakdown characteristics of gases in non-uniform fields are more complicated than in uniform fields, up to now, most of the SF_6/N_2 data are for uniform-field (or coaxial quasi-uniform field) breakdown and for point/plane corona. There are explanations of, and calculations for, uniform and quasi-uniform field cases but no successful calculations or simulations of corona. There is also a lack of information on

corona discharge in SF_6/N_2 gas mixtures. More research needs to be done. In this work, the simulation predicting the steady-state space charge and its effects in positive point/cup electrode system has been developed. The results show that there are two voltages at which streamers appear. They have been proved to correspond to the experimental corona onset and electrical breakdown voltages. The experimental results have confirmed the correctness of the simulation algorithm over much of the pressure range considered. They will be discussed later.

Now, let us discuss the basic streamer production concept and corona phenomena. Also, the onset voltage computation methods will be introduced in detail.

2.2 Breakdown mechanism

2.2.1 The Avalanche

All discharges begin with avalanches. If there is an electron in the gap between two plane parallel electrodes having been emitted from the cathode or released by radiation, it will be accelerated towards the anode. It will collide with gas molecules and there will usually be elastic collisions. But if the electron has gained enough kinetic energy (i.e. energy greater than the ionisation energy of the gas molecule), there is a possibility that the electron will ionise the gas molecule. This is known as 'molecular impact ionisation by electrons'. The result of an ionising collision is the production of a further electron and of a positive ion. The former is accelerated towards the anode and may cause further ionising

collisions. The latter being far heavier is accelerated relatively slowly towards the cathode. The drift velocity of the electrons is at least ten times faster than that of the positive ions. This mechanism results in a 'avalanche' of positive ions and electrons spreading across the gap.

2.2.2 The Streamer Theory

The theory was developed to explain the extremely fast times to breakdown which occur when voltages higher than the minimum breakdown voltage are suddenly applied. These times cannot be explained by the original Townsend theory of breakdown [2] which describes successive waves of avalanches crossing the gap, implying times to breakdown of several times the time to cross the gap. For high over-voltages, the $\exp(\alpha d)$, avalanche multiplication factor is so great that an electron train builds up in a very short distance to be an avalanche without significant diffusion. Very high electron densities cause very high photon production (photoelectrons are produced by photons emitted from the densely ionised gas constituting the avalanche [8]) and local field distortion. Consequently electron avalanches are produced both ahead, and in the tail region, of the original avalanche and the gap becomes 'bridged' by a line of avalanches. This becomes a conducting column very quickly and breakdown occurs.

Therefore, the streamer mechanism is applied in the explanation of the breakdown process in a point/cup system due to the electric field distribution across the electrode gap.

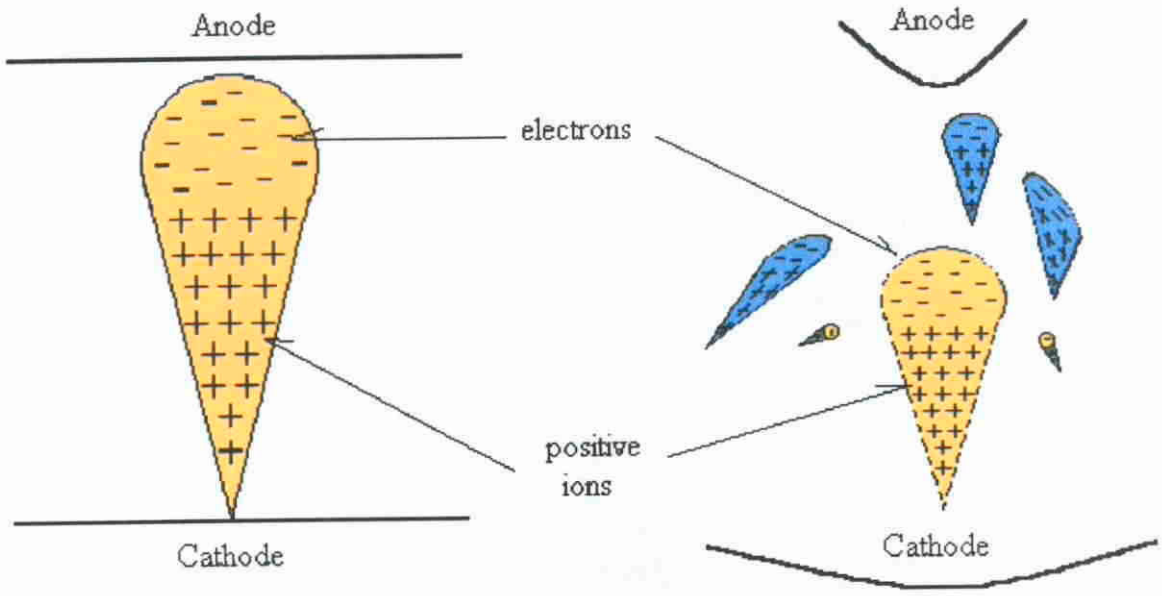

i) Avalanche process *ii) Streamer breakdown process*

Figure 2.1 : The Townsend and Streamer breakdown mechanisms

2.3 Corona discharge concept

Up to now, we have neglected the fundamental quantified and stochastic nature of electrons and electron multiplication, except by noting that a streamer started by one electron might contain 10^9 or more charged particles, enough to cause a measurable current pulse, and lead to breakdown in the uniform-field case. The feedback processes are stochastic as well, and this makes it quite probable that trains of avalanches will die out, even at voltages a little above corona self-sustainment or onset.

Around onset, corona currents thus show very erratic behaviour because they are made up of occasional current pulses due to single streamers. Above the corona onset, after

the appearance of the first successful seed electron, mixed with larger pulses caused by initial enhancement and subsequent reduction of mobility due to space charge accumulation and drift, after long current pauses while we wait for space charges to clear away and new electrons to appear in the ionisation region, quite a variety of phenomena are observed as the corona current is increased, depending on the corona polarity and on the gas density and electron attaching properties.

2.3.1 Streamer production in point/cup electrode system

In the point/cup electrode system, electron and ion pairs are created randomly in the gas gap at low pre-onset voltage as the emission currents are small compared with the 'background radiation' currents. For a negative point electrode, there are three regions under corona conditions (as illustrated in Figure 2.2) [2]. They are :

a) an inner region from cathode to r_s,

b) an intermediate region from r_s to r_c,

c) an outer region from r_c to anode,

where r_c is the radius at which ionisation coefficient is equal to attachment coefficient ($\alpha=\eta$).

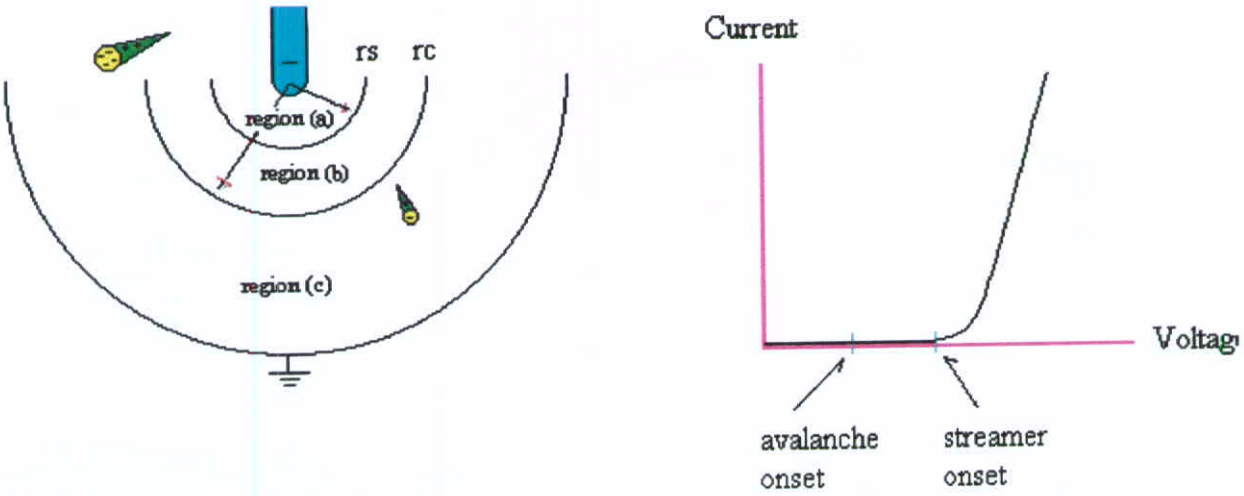

Figure 2.2 : The mechanism of negative corona discharge and its current-voltage characteristics

When the applied voltage increases from zero, the inter-electrode electric field also increases but the attachment coefficient is less than the ionization coefficient ($\alpha<\eta$) throughout the gap. While the voltage reaches to a certain value such that the boundary r_c (where $\alpha=\eta$) is at the negative point electrode, this may be called 'avalanche onset'. With increasing voltage, region (b) appears and increases in its volume until the boundary r_s appears at the negative point electrode, when the situation may be called 'streamer onset'. After that, region (a) appears and increases in its volume until a significant space charge effect is formed. Any 'initial' electron which appears (by ionization caused by radiation or from cosmic rays) in region (a) can transform into a streamer but not in region (b).

In regions (a) and (b), ionisation is more likely than attachment ($\alpha>\eta$) so an electron released there by ionising radiation will accelerate and initiate an avalanche. In region (c) ($r>r_c$), ionisation is less likely than attachment ($\alpha<\eta$) so the electron-head of an

avalanche or streamer entering this region will rapidly decay into negative ions.

Thus an electron released in region (a) will accelerate and initiate an avalanche, which will reach critical size and transform into a streamer before arriving in region (c) where it decays. However an electron released in region (b) ($r_s<r<r_c$) will accelerate and initiate an avalanche which will not reach critical size and hence not transform into a streamer before arriving in region (c).

For a positive point electrode, the situation is reversed for regions (a) and (b) but unchanged for region (c). So electron released will attach in region (c) but form an avalanche which transforms into a streamer in region (b), and in region (a) form an avalanche which strikes the anode before reaching critical size.

2.3.2 Anode corona at static fields

When short voltage pulses are used, there is insufficient time for space charge to drift and accumulate, distorting the original field pattern. Though permitting the creation of space charge as a result of ionising processes, these pulses are not applied long enough to allow space charge to accumulate by drifting in the gap. In this section, we discuss the various activities and manifestations that develop when the voltage is applied for an 'infinitely' long period of time, allowing the created space charge to wander in the field and eventually accumulate to form a steady-state space charge. This will be evident as the discussion of this section proceeds as well as in the treatment of the cathode corona at static

voltage.

In Figure 2.3, the voltages of the typical modes of anode corona are shown as a function of inter-electrode distance, d under air with hemisphere anode [10]. If d is kept constant and the voltage is raised gradually, no detectable ionisation and no conduction current can be observed at first. The very first ionising event, which is extremely faint and can be seen only with a trained eye in a well-darkened room, is a transient. Luminous phenomenon that has the shape of a slightly branched filamentary thread, as illustrated schematically in Figure 2.3.

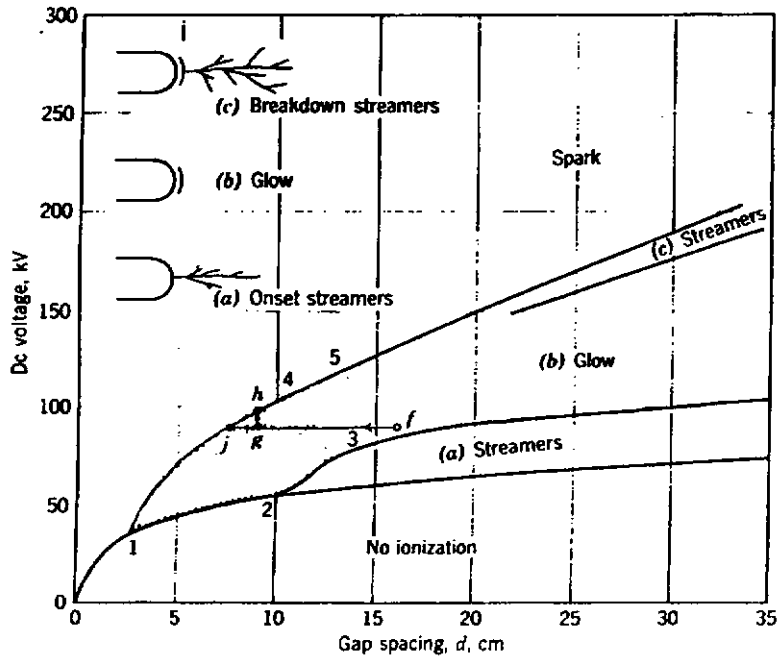

Figure 2.3 : Threshold curves for the various modes of anode corona and for spark breakdown at atmospheric pressure of air [10]

Then a streamer develops with varying frequencies. A streamer gives rise to a

current of magnitude proportional to its physical length. When a streamer happens to be very short, owing to natural statistical fluctuations, it is sometimes referred to as a burst pulse which is in fact nothing else but a streamer.

When the voltage is raised further, streamer occurrence becomes more frequent and tends to be self-sustaining until all transient activities stop and a steady thin glow appears very close to the anode surface. This glow gives rise to a continuous but fluctuating current. The onset and region of existence of this corona mode is shown in Figure 2.3. At an increasing voltage, the current rises and the area of the luminous glow increases both in size and in intensity.

Suddenly, another form of a transient discharge occurs that has the character of a streamer but is more vigorous. These streamers are very bright and cause a distinct acoustic noise. They develop simultaneously with a glow existing very close to the anode. Raising the voltage further, a spark finally materialises and complete breakdown takes place.

2.3.3 Cathode corona at static fields

When static fields, rather than transient fields, are applied to the nonuniform gap with the point negative with respect to the cup, completely different phenomena develop due to the accumulation of ionic space charges by the drift of the ions in the field. Like the anode corona, new field distributions and new corona modes will be the result.

When the voltage across a point-to-cup gap is gradually increased, no ionization occurs and the current is the saturation current (shown in Figure 2.5(b)). At a certain voltage, an abrupt current increase signals the development of streamers, such as regular current pulses (well-known as Trichel pulses).

Figure 2.4 shows the onset voltage of different coronas plotted as a function of electrode separation, d under air with a hemisphere cathode [10]. The lowest curve gives the onset voltage of the Trichel pulses. This onset voltage does not increase very much with d. Raising the voltage will not result in a change of the corona mode for a considerable voltage range. The Trichel pulses or current pulses are due to streamers. Then a new mode of corona appears in which a steady current flows and a glow is observed on the cathode. The onset voltage of this glow is by no means well defined. As the voltage increases, the frequency of the pulses becomes steadily higher and they begin to overlap, eventually appearing as a dc level with a high-frequency ripple. The build-up of space charge eventually lowers the field so that streamers no longer occur – the glow discharge. For this reason this transition is identified by a broad zone, as marked on figure. Above that, the steady-glow corona continues to persist until spark breakdown occurs. In very long gaps, another type of corona is observed between the glow and the spark. This is the negative "streamer", brush or feather.

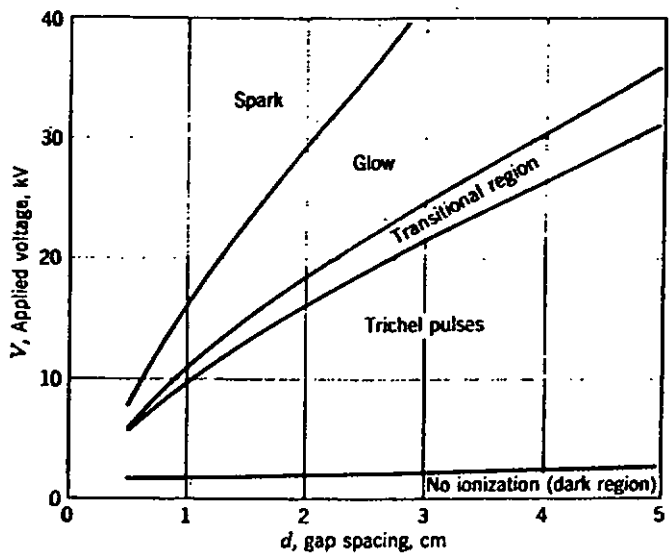

Figure 2.4 : Threshold curves for the various modes of cathode corona and for spark breakdown at atmospheric pressure of air [10]

2.4 Onset voltage computation

A method to predict the breakdown behaviour of SF_6/N_2 mixtures is very desirable. Methods of estimation of the onset voltage (minimum discharge voltage) have been studied. In the simulation, the methods, coefficients and parameters are used so the calculated values can be compared with experimentally measured ones for various mixtures in the pressure range up to 500kPa.

In order to compute the onset voltages of SF_6/N_2 mixtures, an information of effective ionisation coefficient, 'A' should be obtained. 'A' for the mixtures can be calculated from the values of 'A' in pure gases [6].

Effective ionisation coefficient, A = (Ionisation coefficient, α) – (attachment coefficient, η)

For nitrogen, the effective ionisation coefficient can be expressed as [4],

$$A_{N2}/P = 6.6 \exp [-21.5*P/E] \quad (1)$$

where 'P' is the pressure and 'E' is gap electric field.

For sulphur hexafluoride, the effective ionisation coefficient can be expressed as [4],

$$A_{SF6}/P = 27 [E/P - 0.08775] \quad (2)$$

where 'A/P' has the units of $(mm\ kPa)^{-1}$ and 'E/P' has the units of $kV(mm\ kPa)^{-1}$.

(Remarks : 1 bar = 100 kPa)

For the mixtures, the effective ionisation coefficient can be expressed as [4],

$$A_{MIX}/P = Z (A_{SF6}/P) + (1-Z) (A_{SF6}/P) \quad (3)$$

where $Z = P_{SF6}/P_{MIX}$ is the partial pressure ratio of the SF_6 component in a given mixture.

Figure 2.5 shows the variation of 'A/P' as a function of 'E/P' for the mixtures. For our st in the positive effective ionisation coefficient, the region (A/P>0) can be oximated by

$$A/P = \beta [E/P - (E/P)_{lim}] \quad (4)$$

ere 'β' and '$(E/P)_{lim}$' are mixture ratio dependent.

The critical numbers of a streamer for pure SF_6 and pure N_2 are 10^7 and 10^8, respectively [5]. So the critical number for the mixture is assumed to be [5] :

$$N_{MIX} = Z*10^7 + (1-Z)*10^8 \quad (5)$$

where Z is mixture ratio.

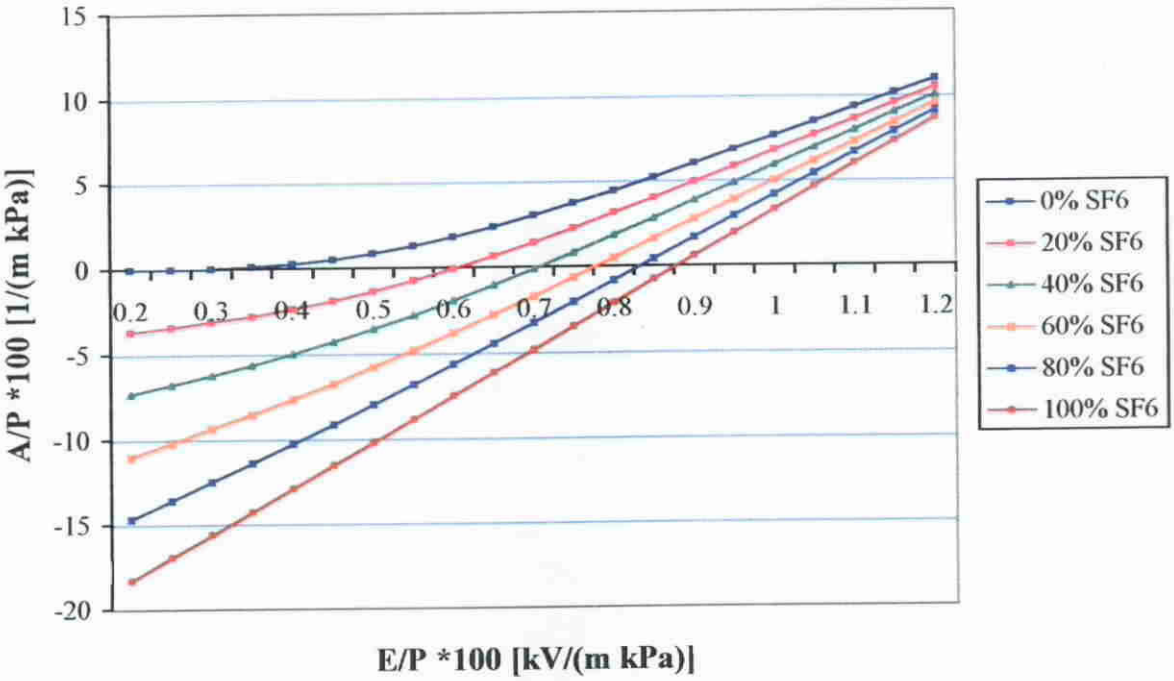

Figure 2.5 : The graph of effective ionisation coefficient per unit pressure, E/P, vs. gap electric field per unit pressure, α/P, for various mixtures of SF_6 and N_2

Point-cup gaps have been used to study the pre-breakdown and breakdown characteristics of SF_6/N_2 in highly non-uniform field gaps. In such gaps, at low pressures, the corona inception occurs first and the breakdown voltage is equal to or higher than the onset voltage. The streamer criterion given by equation (5) should give the corona inception levels at low pressure in such gaps. The effective ionisation coefficients for SF_6/N_2 mixtures can be approximated by a linear relationship in the vicinity of $(E/p)_{lim}$. A simplified streamer criterion proposed for SF_6 can be used to calculate the discharge

inception levels in SF_6/N_2 mixtures. Comparison with the measured values indicates a good agreement over a range of mixture ratios and electrode configuration.

In simple simulation, there are two methods to find out the value of onset voltage. The computer software 'Matlab' and 'Turbo C++' are involved, respectively.

Method 1: by solving non-linear equations by the 'Matlab' software

a) set $A_{MIX} = 0$ from equation (3) to find r_c.

b) find out onset voltage by solving the nonlinear equation : integration of A_{MIX} from radius of point electrode to r_c is equal to natural logarithm of N_{MIX}.

Method 2: by iteration method performed by 'Turbo C++' program (adapted and developed from the method used in [1])

a) advance its path from surface of point electrode by step until a point where $\alpha=\eta$ is reached. This path length is r_c.

b) sum up all A*d from surface of point electrode to r_c until the value is larger than natural logarithm of N_{MIX} where d is path step.

This also neglects space charge.

However this assumes the absence of space charge, such calculations give onset voltage far below the measured values, so it must be assumed that space charge is present.

Turbo C++ program will be mainly applied to simulate the onset voltage and also

the breakdown voltage of corona discharge in the point-cup system under various parameters including pressure, mixture ratio, etc. as discussed in later chapters. In order to consider the effect of space charge on the field, that is by applying Poisson's equation rather than Laplace's, a more complex program must be developed. This is the major intention in the present work.

Chapter 3

Experimental Setup

Chapter 3 - Experimental Setup

The experimental equipment setup is shown in Figure 3.1. It is a standard circuit for high direct voltage generation and measurement. The electrode system was housed in a cylindrical pressure vessel which was evacuated before pressurising with SF_6 and N_2. The point/cup electrode system is illustrated in Figure 3.2. It comprises a copper hemispherical pointed electrode (diameter=1.5, 3 or 6 mm) concentric with a copper hemispherical concave electrode (radius=30 mm).

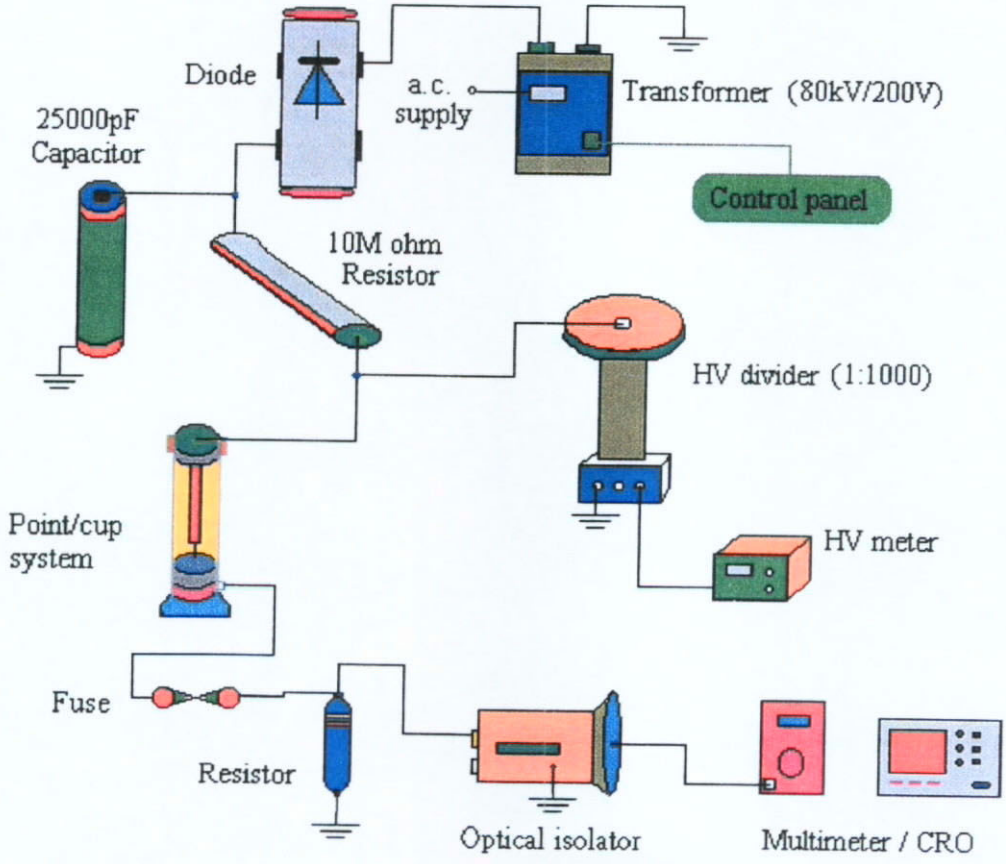

Figure 3.1 : The experiment equipment and circuit

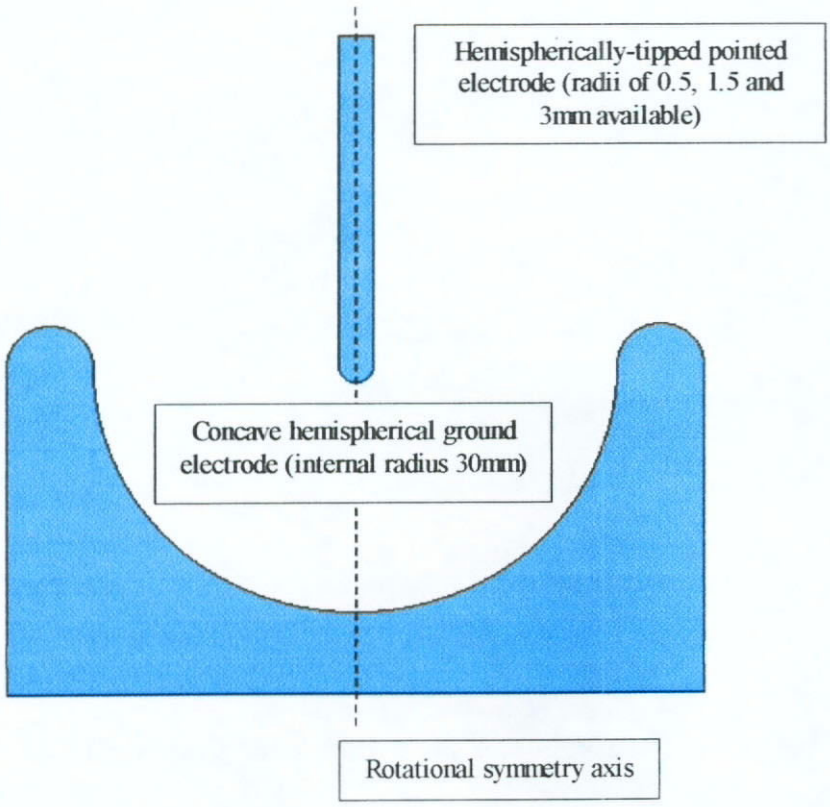

Figure 3.2 : The point/cup electrode system

Both positive and negative direct voltages were applied to the pointed electrode through the smoothed rectified ac supply. The gap currents were measured as the potential difference developed across a 10K-ohm series resistor ('R' in Figure 3.3) in the earth lead of the cup electrode. This potential was measured by a digital multimeter via an optical isolator system consisting of a transmitter unit, an optical fibre and a receiver unit which was used to protect the measuring instrument against injury during breakdown. The circuit is illustrated in Figure 3.3. When the onset voltage was measured, the multimeter was replaced by a digital storage oscilloscope (DSO) which allowed the start of pulses to be

observed.

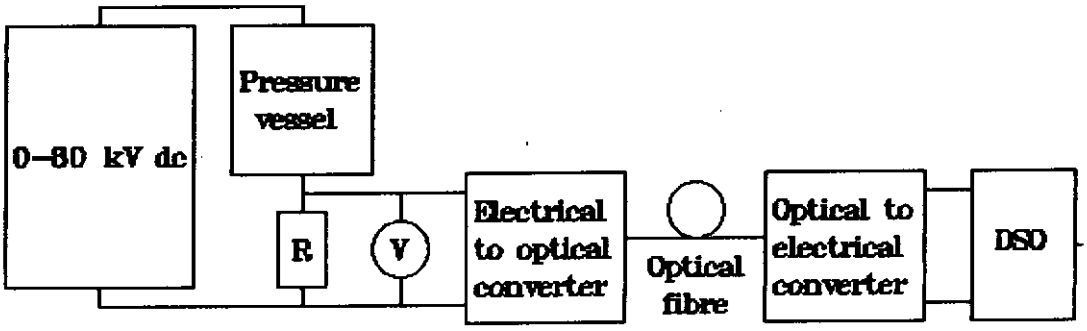

Figure 3.3 : The block diagram of experiment circuit

The experimental work involved the measurement of onset and breakdown voltages under various pressures between 0.5 and 5 bar, various point electrode diameters between 1.5 mm to 6 mm, various mixture ratios between pure SF_6 and N_2. Positive, negative and ac corona results were recorded. 3 times of each experiment under the specified parameters have been done. The average values of those results were recorded for analysis. The results will be discussed and analyzed in the following chapters.

Chapter 4

Experimental Results and Discussion

Chapter 4 - Experimental Results and Discussion

The experimental results of SF_6/N_2 corona discharge are described, analysed and explained.

4.1 Effect of mixture ratio on positive, negative and AC onset voltages

Figure 4.1 shows the measured onset and breakdown voltages for a range of SF_6/N_2 mixtures at a pressure of 1 bar. It also shows that the positive onset voltage is a little more than the negative one. It is believed that only dc voltage level raised is observed in CRO during positive onset rather than shape pulse observed during negative one. So it is difficult to locate the positive onset point accurately.

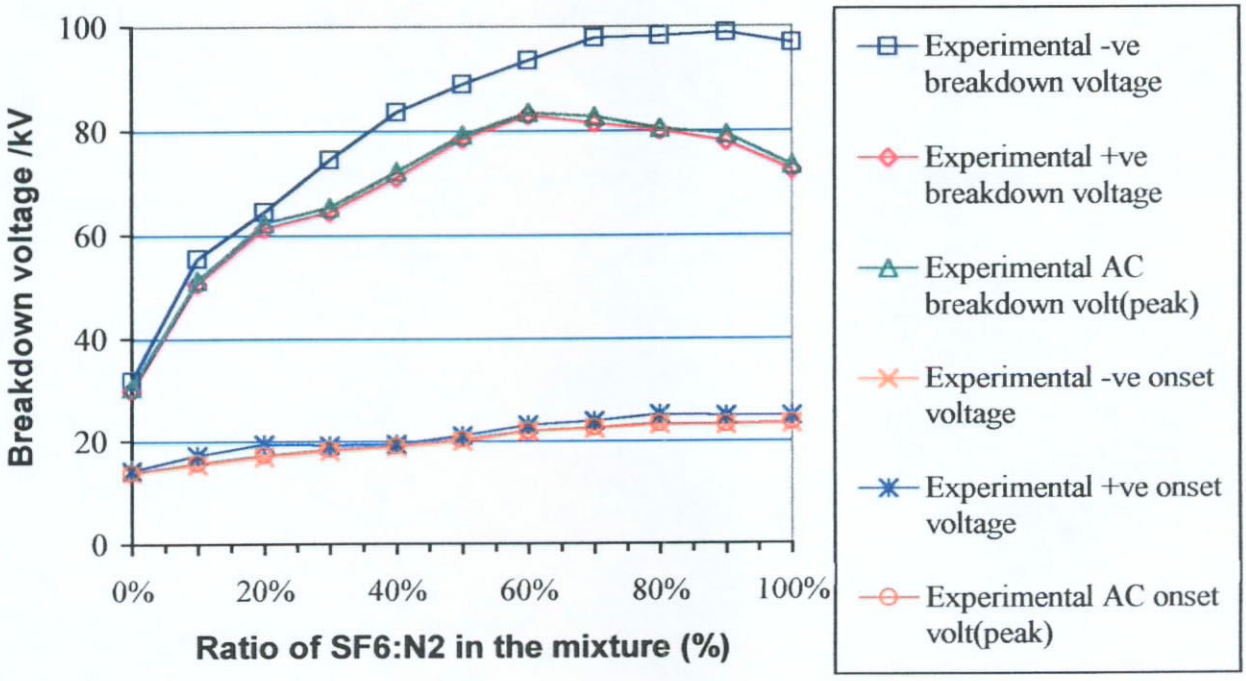

Figure 4.1 : The graph of experimental onset and breakdown voltage vs. SF_6/N_2 mixture ratio under 1 bar pressure and 3mm diameter point electrode

When the frequency of the applied field is 50 Hz (period between field polarity reversals is 10 msec.), the polarity of the electrodes will change very slowly as compared with the breakdown process, which is completed in intervals of 10^{-6} to 10^{-8} s, the alternating voltage will not have enough time to reverse the direction of the electric field once the breakdown process has been initiated [4]. The mechanism is essentially the same as under steady fields. The only effect will be that the ionisation in the gas will be subject to a slowly varying field. If the voltage magnitude reaches onset value during the voltage peak, then electron avalanches will be produced in the same way as under constant field. So the peak AC onset voltage is expected to be equal to the negative onset voltage since the negative onset is lower than the positive onset voltage. This is seen to be the case in Figure 4.1.

4.2 Effect of pressure on onset voltage

As the inter-electrode pressure increases, the actual path of electrons before making a successful collision is shorter. So higher electric field is required for avalanches and streamers to occur. Basically 'α' slightly greater than 'η' is the criterion for ionisation to occur. This occurs at E=8.775 kV/mm for pure SF_6 content at 1 bar. So critical electric field is equal to 8.775P kV/mm. For given geometry, voltage is proportional to pressure.

In Figures 4.2 and 4.3, it shows that the experimental results of negative and positive corona are similar up to 2 bar pressure. For pressure larger than 2 bars, where the onset voltages mostly exceed 40 kV and hence electric field close to the negative point

electrode is above about 250 kV/cm, field-enhanced emission probably occurs [11]. Thus there is a large supply of electrons and more numerous avalanches occur, leading to an accumulation of charges near the point. So onset voltage is found to be around 40 to 50kV and cannot rise further. On the other hand, the onset voltages of positive corona larger than 3 bar pressure drop with pressure increase. But the reason is unknown. To sum up, onset voltages of positive corona is a bit higher than the negative ones only for pressure up to 2 bars and stops to increase at higher pressure.

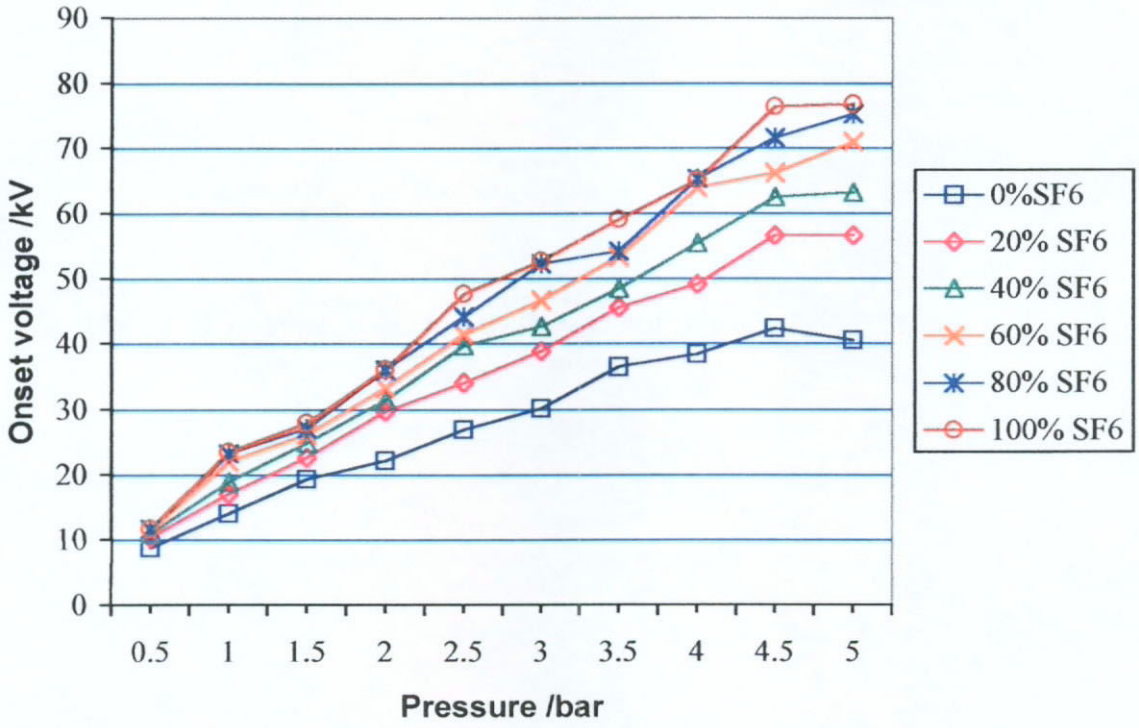

Figure 4.2 : The graph of experimental negative onset voltage vs. pressure under various gas mixture ratios with 3mm diameter point electrode

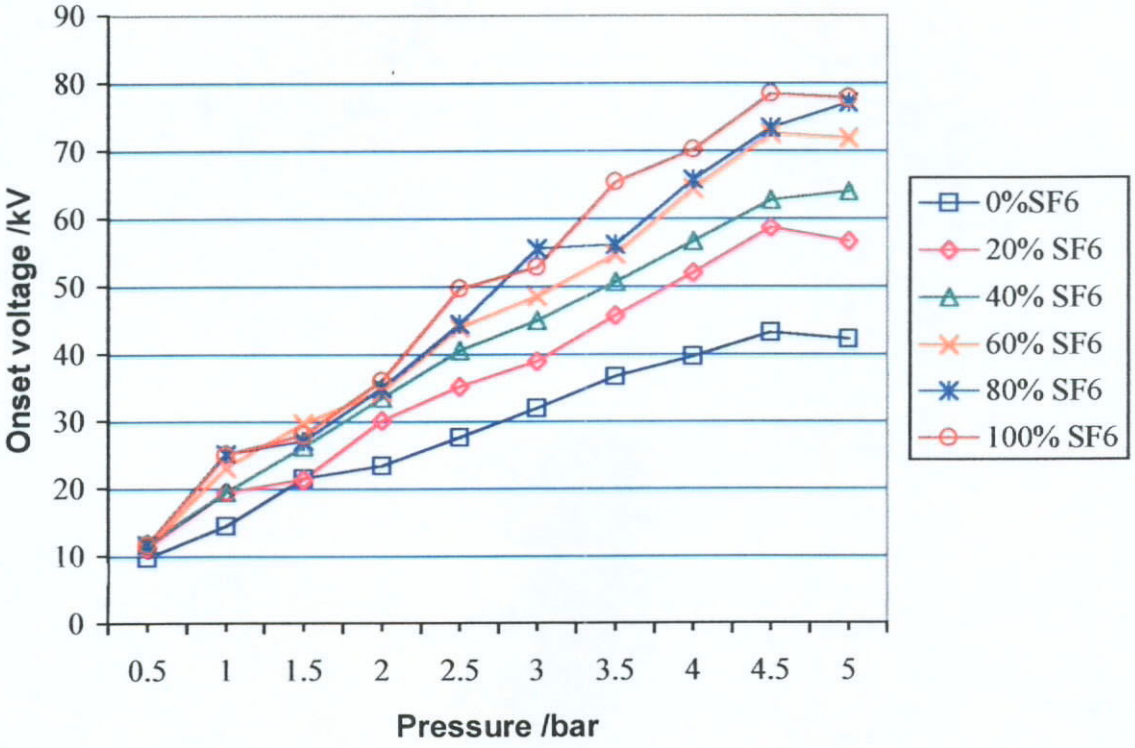

Figure 4.3 : The graph of experimental positive onset voltage vs. pressure under various gas mixture ratios with 3mm diameter point electrode

4.3 The effect of pressure on breakdown voltage

In Figure 4.4, the graph of experimental onset and breakdown voltages against pressure is illustrated. The results show that the experimental breakdown voltage curves run far away from onset voltage curves for both cases (pure SF_6 and pure N_2) at lower pressure. At higher pressure, the experimental breakdown voltage curves will be close to the onset voltage curves.

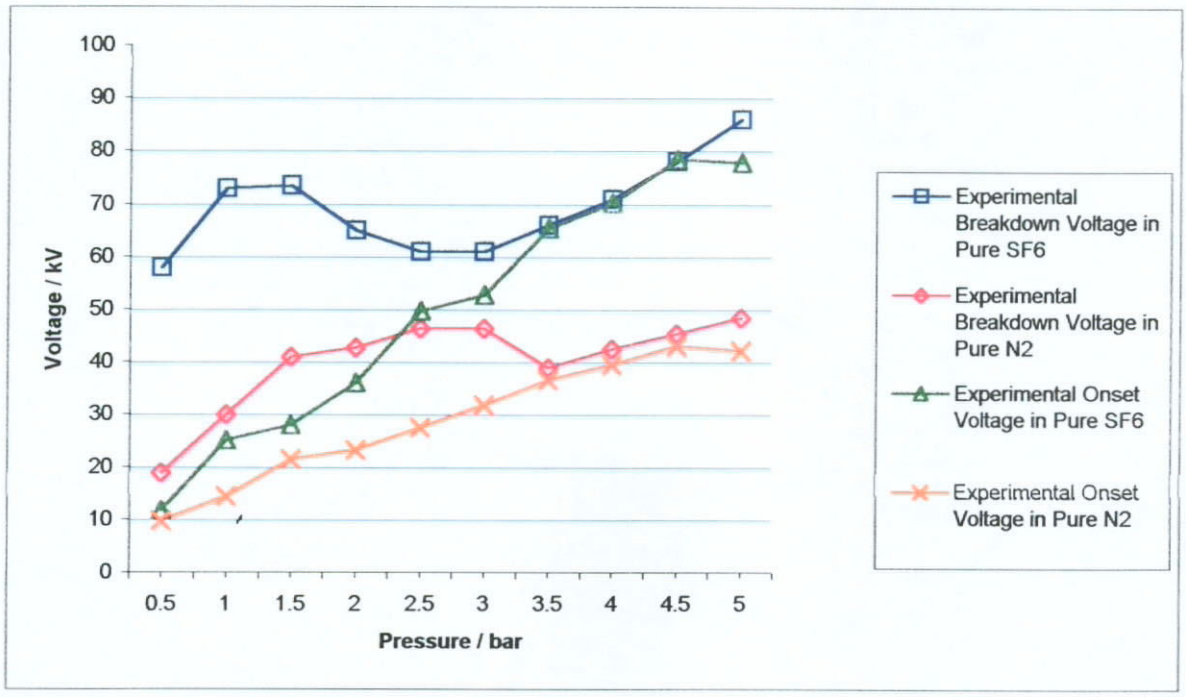

Figure 4.4 : The graph of experimental positive onset and breakdown voltages vs. pressure at pure SF_6 and N_2 with 3mm diameter point electrode

For pressure lower than 3.5 bar, due to the accumulated positive ion cloud near the point, E-field near the point surface reduces and breakdown occurs at a much higher value. For pressure higher than 3.5 bar, at onset voltage value, the E-field near the point surface is so high that the streamers can be formed in a short distance. The ions move towards to the cup electrode and repel against each other at the same time. Eventually, the positive ion cloud near the point cannot be formed and the avalanche of the electrons can form a streamer (because of enough $K=\int Adr$ value – 16.4 for SF_6).

On the other hand, I found that for pure N_2, due to only ionization rate is less than SF_6, less space charge effect exists although initial electron starts near the cup electrode

for positive corona, it will reach the point with a similar avalanche size to 'non-space charge effect' one.

For pure SF_6, because ionization region exists near the point and attachment region exists at other region, if space charge exists, it always reduces the electric field near the point electrode (ionization region) and increases it near the cup electrode (attachment region). So the avalanche size at ionization region will be less than the 'non-space charge' one. To sum up, space charge effect exists in SF_6 but less in N_2.

For pure N_2 at 1-bar pressure (3mm diameter point, positive and negative corona), onset voltage is about 15kV and breakdown voltage is about 30kV. So there is some difference between onset and breakdown which is due to the little space charge effect. For pure SF_6, there is a large difference due to large space charge effect.

For pure SF_6 at 3-bar pressure, the breakdown voltage for positive corona is much lower than for the negative corona one; and there is a large difference between the onset and breakdown voltages. For 4-bar pressure, the difference becomes smaller. For 5-bar pressure, the difference is close to zero.

Because at the onset voltage of 3-bar pressure for positive corona, the boundary of ionization region in inter-electrode gap becomes close to the point electrode. Also, the ionization path becomes shorter. Only a little amount of space charge starts to be formed near the point surface. Because less positive ions accumulate near the point electrode to

produce a significant space charge effect. Also, the space charge cloud cannot stay for a long time and disappear (drift out from point) very fast. But due to continuous avalanches and streamers formed, space charge cloud still exists but provides a weaker effect only. So the difference between onset and breakdown voltage is reduced.

For the same reason, at 5-bar pressure for positive corona, the boundary of ionization region becomes close the point. Also at onset voltage, only a smaller amount of space charge is started to be formed near point surface. The very high E-field in this region means a short ionization path. Also, the space charge cloud cannot stay for a long time and disappear very quickly even continuous avalanches and streamers are formed. So space charge effect is almost eliminated. The difference between onset and breakdown voltage is nearly zero.

For the case of negative corona, the space charge cloud always starts at a region near '$\alpha=\eta$' boundary rather than near the point surface. Because the E-field at the region near the '$\alpha=\eta$' boundary is lower than that of the point surface, the drift velocity of negative ions is also lower. So the space charge cloud drifts away quite slowly and the continuous streamers and avalanches formed keeps the space charge cloud exist. Therefore, the difference between onset and breakdown voltage is always large.

4.4 Current-voltage characteristics of corona discharge

The pre-corona measurements follow the empirical parabolic Townsend

relationship closely [2]

$$I = kV(V - V_o)$$

where V_o is the corona onset voltage, and k is a constant.

Figures 4.5-4.15 also show the graphs of experimental current-voltage characteristics of corona discharge under various gas mixture ratios with different pressures and sizes of point electrode. In Figures 4.14 and 4.15, due to the smaller diameter of point electrode, onset voltage should be very low and the spark breakdown voltage is high. i.e. the transition region is wide because the gap electrode field is quite non-uniform in this case.

There is a discontinuity at the onset voltage of the measured results. Because the corona current is composed of small pulses (streamers), which may be as much as a second apart, the digital multimeter, DMM will always miss some pulses due to its sampling nature. Just above the onset voltage, the 'sample' taken by the DMM may contain, for example, either 2, 3 or 4 pulses; consequently the reading of (average) current on the DMM will fluctuate between current readings corresponding to 2, 3 or 4 pulses. This effect may result in errors unless an analogue voltmeter is used for these readings. Thus the onset voltage point should be checked by digital stored oscilloscope (DSO) or CRO rather than DMM. Also, this point can be located by extrapolation of the 'corona current vs. voltage' curve.

In the negative-point electrode, there is a large supply of electrons due to field-enhanced emission at the higher voltages so that avalanches develop near the point. 'Higher voltages' in this context mean above 40kV for a 3-mm diameter electrode. But the electrons continue to travel across the gap to the positive plane without further ionisation occurring. It is suggested that this causes a large amount of positive space charge to shield the point so that the gap field is greater very close to the surface of the point but is lower further away. Thus a higher breakdown voltage is required than in the positive-point case [1].

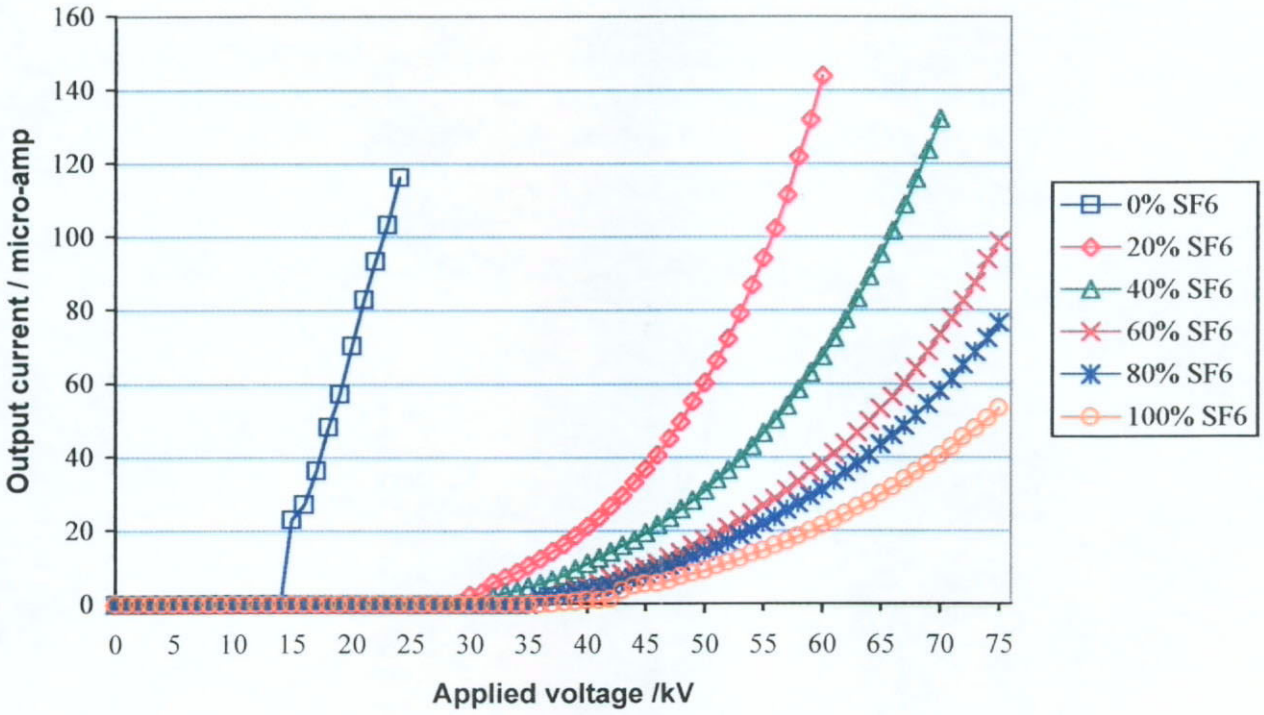

Figure 4.5 : The graph of experimental current-voltage characteristics of negative corona discharge under various gas mixture ratios with 1 bar pressure and 6mm diameter point electrode

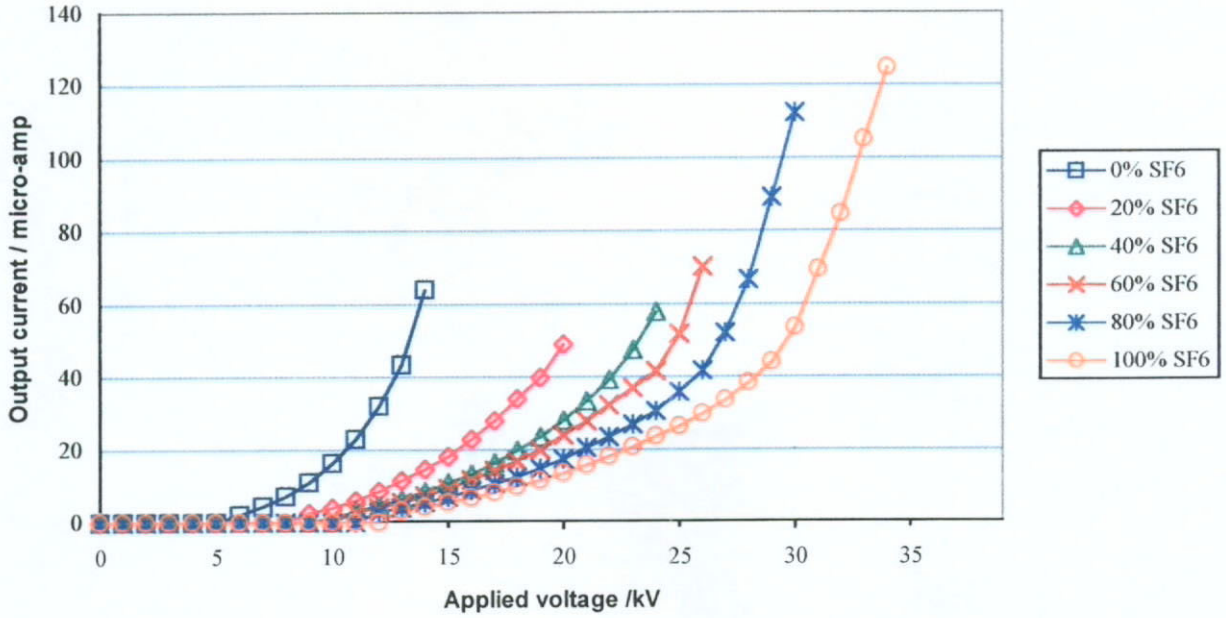

Figure 4.6 : The graph of experimental current-voltage characteristics of negative corona discharge under various gas mixture ratios with 0.2 bar pressure and 3mm diameter point electrode

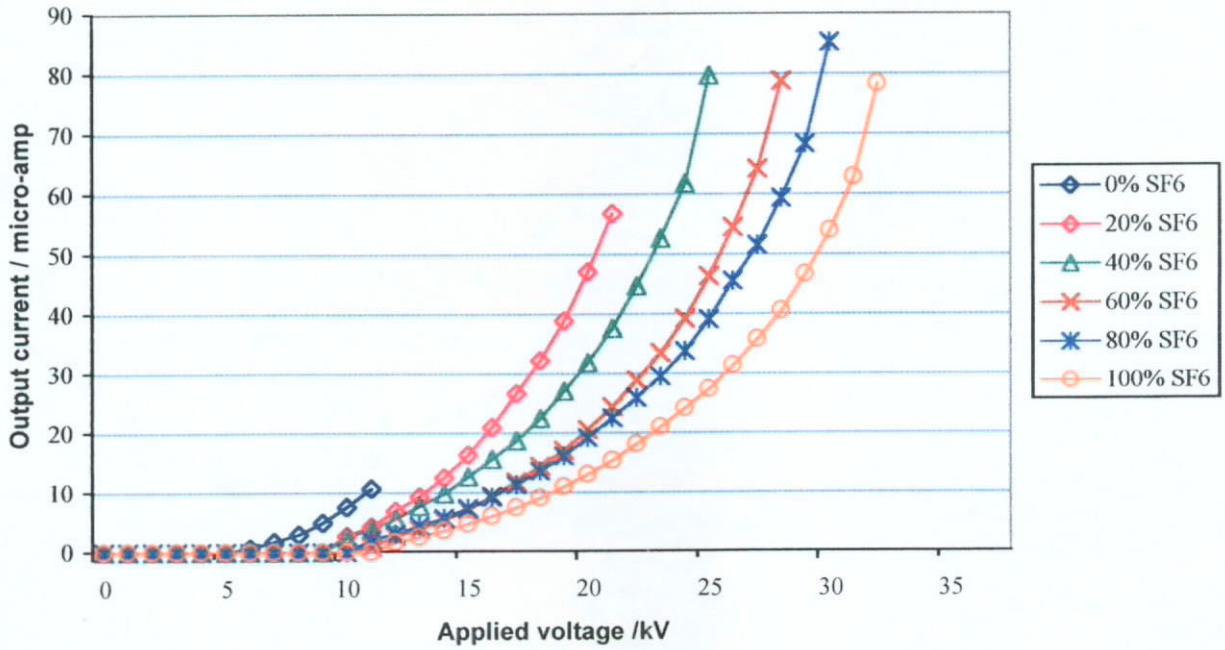

Figure 4.7 : The graph of experimental current-voltage characteristics of positive corona discharge under various gas mixture ratios with 0.2 bar pressure and 3mm diameter point electrode

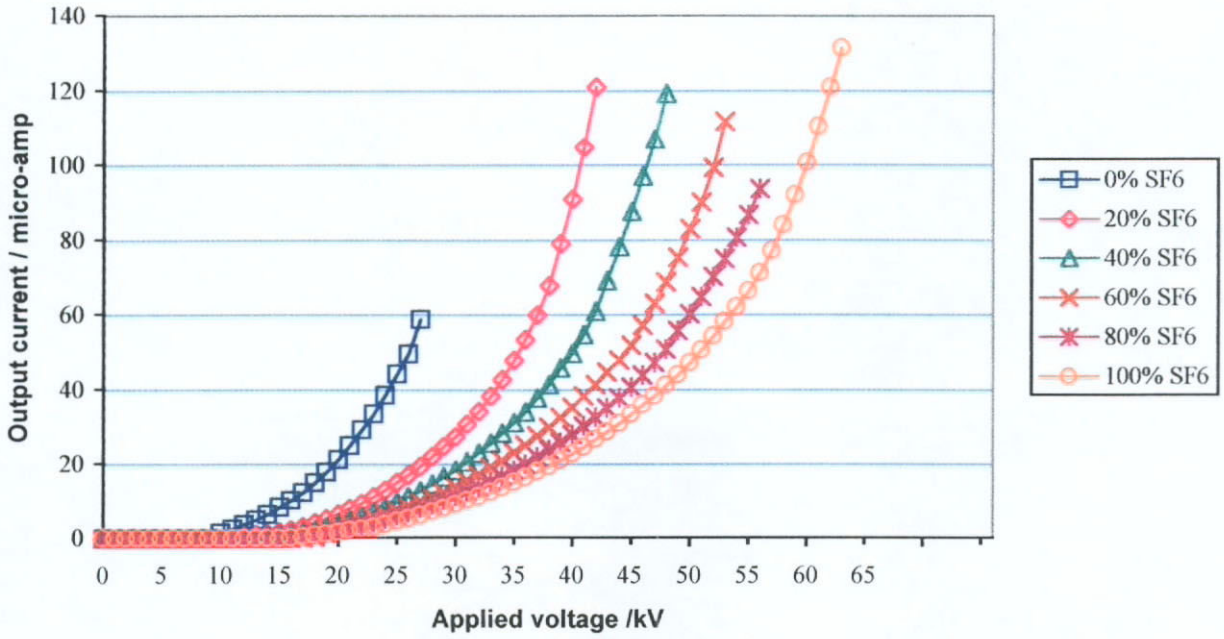

Figure 4.8 : The graph of experimental current-voltage characteristics of negative corona discharge under various gas mixture ratios with 0.5 bar pressure and 3mm diameter point electrode

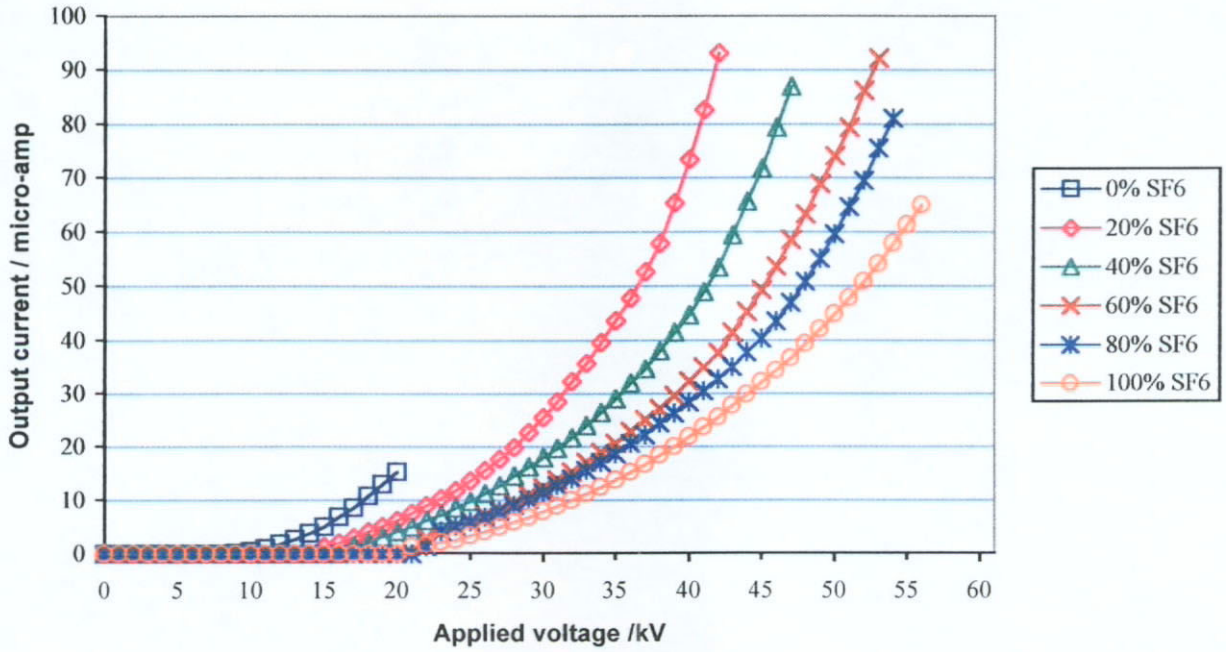

Figure 4.9 : The graph of experimental current-voltage characteristics of positive corona discharge under various gas mixture ratios with 0.5 bar pressure and 3mm diameter point electrode

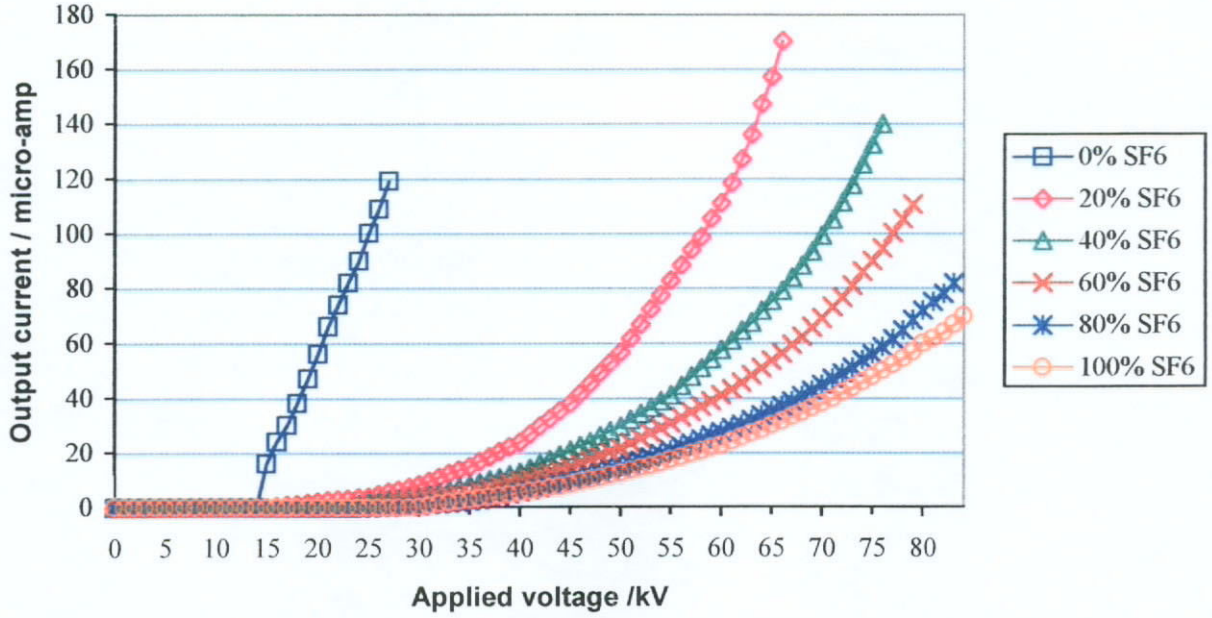

Figure 4.10 : The graph of experimental current-voltage characteristics of negative corona discharge under various gas mixture ratios with 1 bar pressure and 3mm diameter point electrode

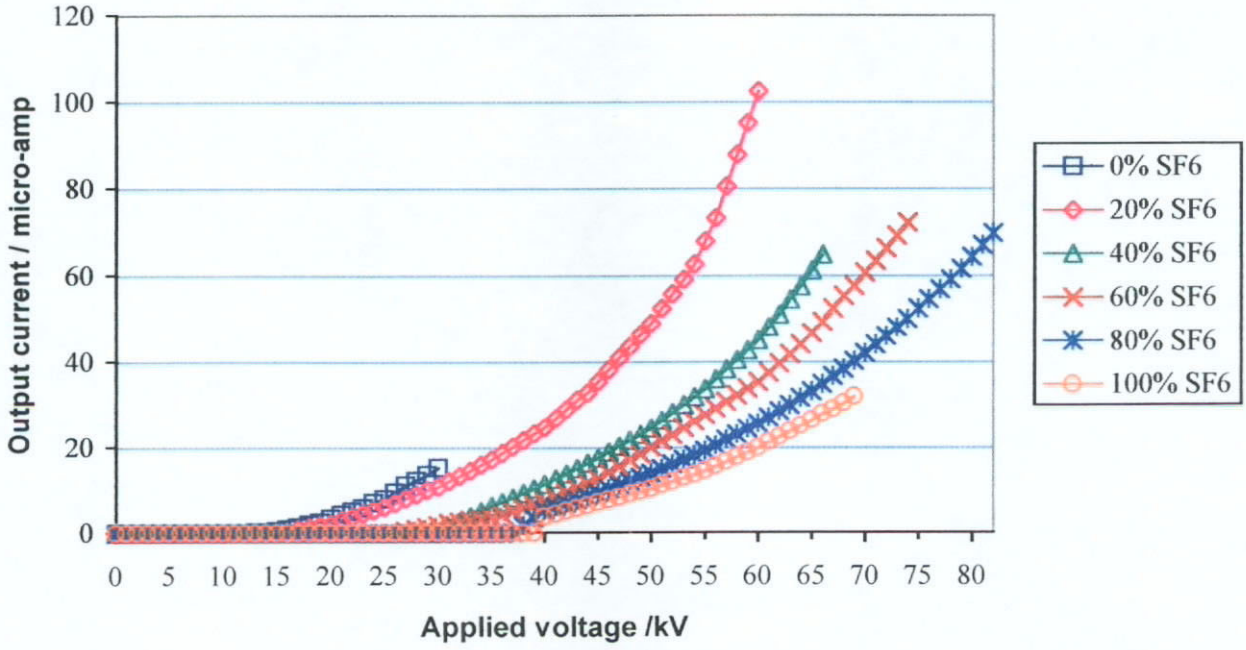

Figure 4.11 : The graph of experimental current-voltage characteristics of positive corona discharge under various gas mixture ratios with 1 bar pressure and 3mm diameter point electrode

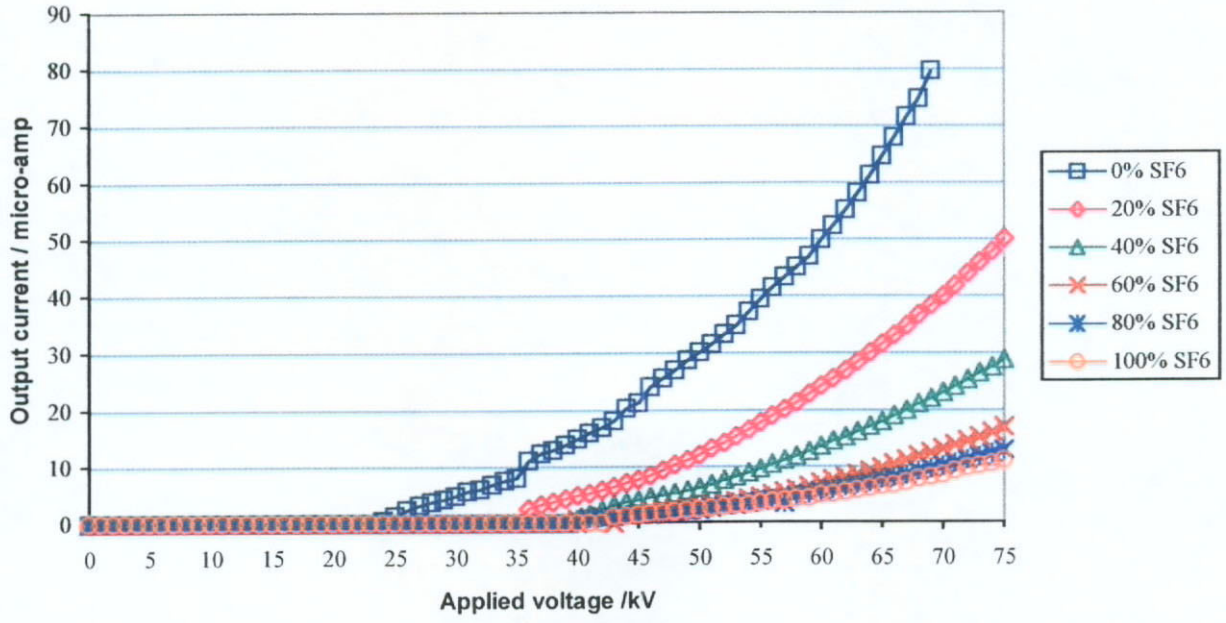

Figure 4.12 : The graph of experimental current-voltage characteristics of negative corona discharge under various gas mixture ratios with 2 bar pressure and 3mm diameter point electrode

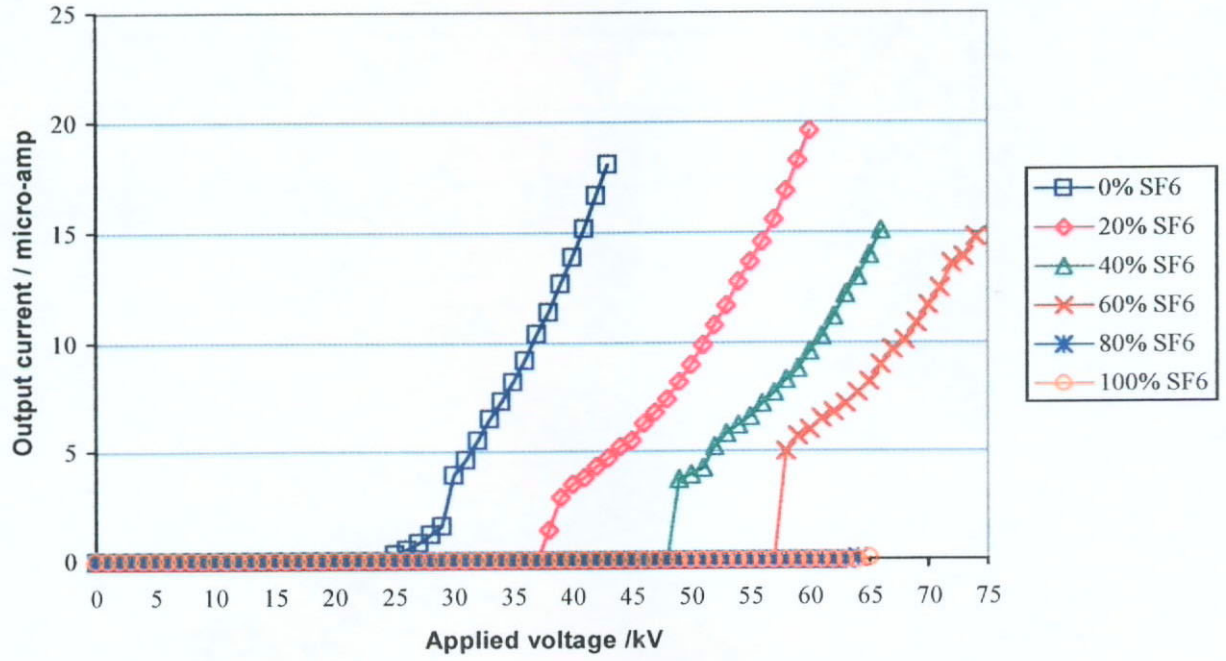

Figure 4.13 : The graph of experimental current-voltage characteristics of positive corona discharge under various gas mixture ratios with 2 bar pressure and 3mm diameter point electrode

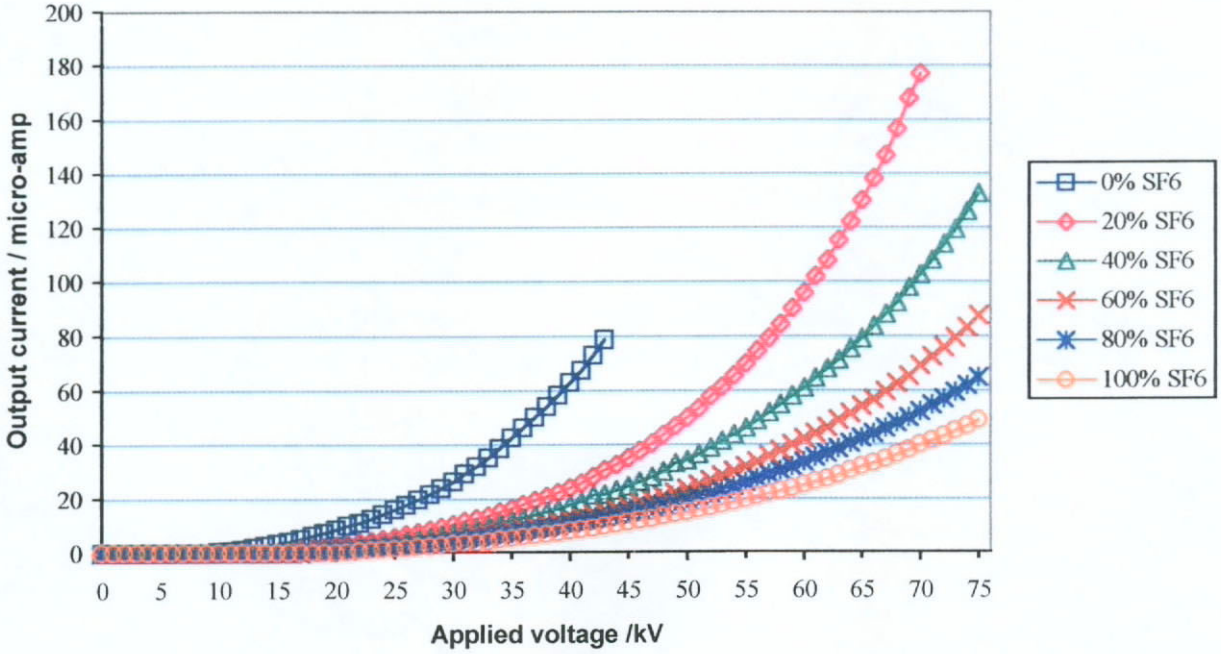

Figure 4.14 : The graph of experimental current-voltage characteristics of negative corona discharge under various gas mixture ratios with 1 bar pressure and 1.5mm diameter point electrode

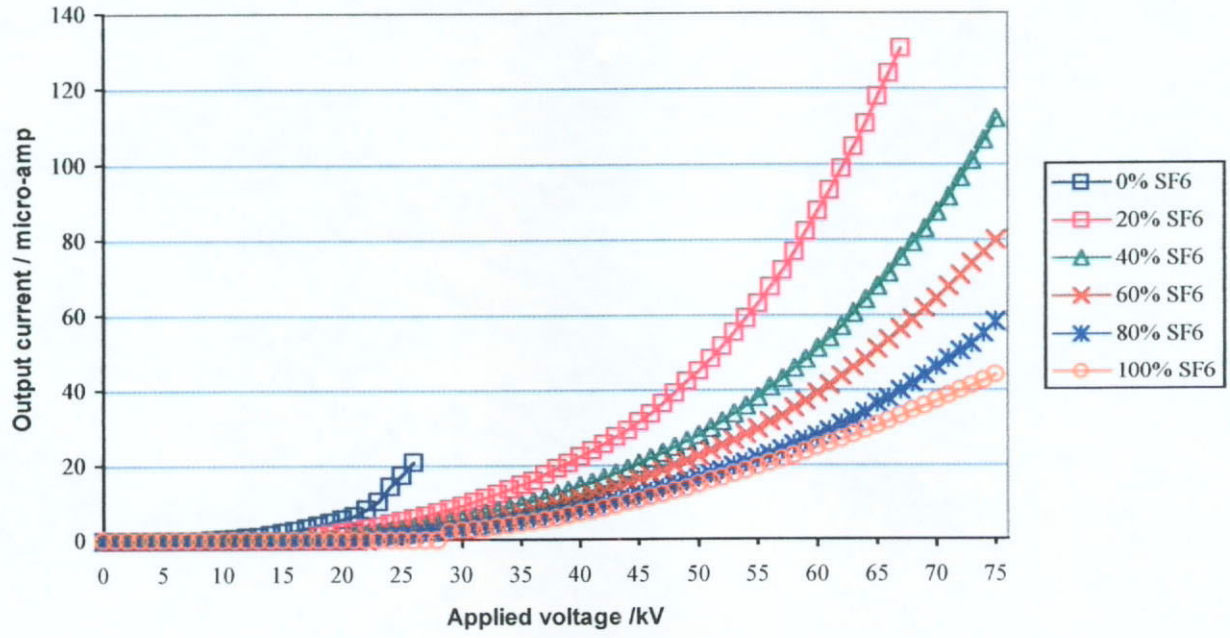

Figure 4.15 : The graph of experimental current-voltage characteristics of positive corona discharge under various gas mixture ratios with 1 bar pressure and 1.5mm diameter point electrode

4.5 Effect of point electrode diameter on onset voltage

As the radius of the point electrode increases, the Laplace electric field near the point surface where ionization occurs significantly decreases. So it becomes difficult to ionise the electrons near the point under the same applied voltage. The number of avalanches and streamers will become less. Onset voltage should be increased to increase the volume of region '$\alpha > \eta$' for ionization. To sum up, onset voltage increases with the radius of point electrode. In Figure 4.5, it shows the experimental results of the negative corona discharge with 6mm diameter point electrode. The onset voltages are higher than those using 1.5mm and 3mm diameter point electrode.

Chapter 5

Space Charge Simulation

Chapter 5 - Space Charge Simulation

5.1 Introduction

In positive corona, for each avalanche, positive ions are remained behind. The drift velocity of positive ion is much less than that of the electron. So positive ions stay and accumulate in the inter-electrode gap after the electrons have reached the electrode. After several large avalanches, there are a lot of accumulated positive ions in the space and producing a reversed electric field to the original Laplace field. So the motion of electrons is opposed. This space charge effect becomes significant when the applied voltage is much higher than the onset voltage. The breakdown characteristics of SF_6/N_2 corona discharge is affected. As a result, spark breakdown voltage becomes much higher than onset voltage at high SF_6 content. Also, the shape of 'corona current vs. voltage' changes. And this effect accounts for the difference between positive and negative results. To sum up, we need to consider space charge in the simulations.

Due to the fact that there are many avalanches appearing at different locations at the same time, one avalanche space charge simulation is unreal if dc voltage is applied. However the exact locations of avalanches are unknown. So it is not possible to simulate the space charge accurately by assuming the locations and frequencies of avalanches. Obviously, a steady-state will be reached when a constant voltage is applied because the output current reading is constant. So it is believed that a constant gap electric field profile will be obtained during steady-state situation and also for space charge profile.

In the space charge simulation, 'Turbo C++' is used to write and execute the algorithm models of both positive and negative corona discharges. For positive corona, we consider the positive ion effect only as SF_6^- ions are in the majority in low field zone but SF_6^+ ions are in a majority near the point electrode (where the field is high and most ionisation takes place). So the simulation can be simplified by taking this assumption.

For negative corona, we consider the negative ions and electrons only. But we also consider the positive ions near the point. Because SF_6^+ ions move towards the point electrode and then disappear. They affect the local electric field near the point. And the SF_6^- ions accumulated at the ionisation boundary (where $\alpha=\eta$) also provide a considerable space charge effect in the inter-electrode gap.

In the simulation, we try to divide the inter-electrode gap into several zones. In the ionisation region (effective ionisation coefficient larger than zero), each zone is 0.001cm wide and in the attachment region (effective ionisation coefficient less than zero), we define the ions and electrons here provide a neglected space charge effect. Therefore the total number of zones calculated depend on the applied voltage, pressure and gas mixture ratio. In each zone, the resultant number of positive ions/negative ions/electrons is equal to the number of positive ions/negative ions/electrons drifting in plus the number of positive ions/negative ions/electrons created minus the number of positive ions/negative ions/electrons drifting out the zone. In each iteration, the time is advanced by step and the resultant number of positive ions is calculated from the parameters. Then resultant local electric field on each zone can be updated each time as the space charge electric field

depends on the ion and electron density distribution in all zones. The whole process repeats until the value of the resultant number of positive ions in each zone converges. This convergence represents that the steady-state situation can be reached. The iteration ends. The flowchart of the algorithm is shown in Figure 5.1.

However, the program has some limitations. They include less zones divided and large time step. So they restrict the range of applied voltage, pressure and SF_6/N_2 mixture ratio in the application. It means that if these parameters are out of their ranges, no convergence is obtained, i.e. no steady state situation can be simulated. Also, the program gives a rough estimation of space charge effect only because the real discharge process involved is not simple.

5.2 Program algorithm

The algorithm of space-charge simulation for SF_6/N_2 mixture positive corona discharge is based on the following steps. It should be emphasized that the program attempts to derive the steady-state situation on a continuous ionisation basis whereas the streamers are discrete occurrences and each raises the positive ion density at its location as a significant increment. There is thus a continual fluctuation in space charge density.

a. Input the parameters

This includes the applied voltage, pressure, ratio of mixture and pointed electrode radius. Divide the ionization region into zones with zone width 0.001cm.

b. Calculate the Laplace electric field and hence effective ionization coefficient in all zones

In the hemisphere electrode system, Laplace electric field at a distance x from the centre,

$$E[x] = V*R_p*R_c/(R_c-R_p)/x^2$$

where 'V' is applied voltage, 'R_c' is cup electrode radius, 'R_p' is pointed electrode radius.

Effective ionisation coefficient, A = (Ionisation coefficient, α) – (attachment coefficient, η)

For nitrogen, the effective ionisation coefficient can be expressed as,

$$A_{N2}/P = 66 \exp [-2.15*P/E]$$

where 'P' is the pressure and 'E' is gap electric field.

For sulphur hexafluoride, the effective ionisation coefficient can be expressed as,

$$A_{SF6}/P = 27 [E/P - 0.8775]$$

where 'A/P' has the units of $(cm\ kPa)^{-1}$ and 'E/P' has the units of $kV(cm\ kPa)^{-1}$.

(Remarks : 1 bar = 100 kPa)

For the mixtures, the effective ionisation coefficient can be expressed as,

$$A_{MIX}/P = Z\,(A_{SF6}/P) + (1-Z)\,(A_{SF6}/P)$$

where $Z = P_{SF6}/P_{MIX}$ is the partial pressure ratio of the SF_6 component in a given mixture.

c. Find out the size of ionization region and hence calculate the number of zones required

Search the ionization boundary where $A_{MIX} = 0$.

d. Find out suitable time step

Set a fixed maximum time step, t so that the maximum drift distance of ions or electrons will not exceed the zone size (0.001cm).

e. Set the time zero and start at the zone near the pointed electrode

f. ***Find out drift velocity of ions and electrons in each zone***

$$v = \mu E$$

where 'v' is drift velocity and μ is mobility.

g. Find out the number of electrons created from background radiation in each zone

We assume that the production rate of an initial electron from background radiation is $5x10^{12}$ per second per cubic centimeter and emission rate of electron from negative point electrode is $1x10^{16}$ per second per cubic centimeter [10].

h. Calculate drift distance and number of electrons and ions drifting in and out of the zone

Drift distance of ions or electrons, d = v t

Number of electrons drifting in/out = 100*Ne[t]*d

where 'Ne[t]' is existing number of electrons. Calculation for positive and negative ions is similar.

i. ***Test the zone whether ionization or attachment occurs there and hence calculate the number of electrons and positive /negative ions formed***

Number of new electrons produced in ionization region = Ne[t]*exp(A_{MIX} d)

Number of new positive ions produced in ionization region = Ne[t]*exp(A_{MIX} d)

Number of new negative ions produced in ionization region = 0

Number of new electrons produced in attachment region = -Ne[t]*exp(-A_{MIX} d)

Number of new positive ions produced in attachment region = 0

Number of new negative ions produced in attachment region = Ne[t]*exp(-A_{MIX} d)

where 'Ne[t]' is existing number of electrons and 'd' is drift distance of electrons in the specified time step in the zone.

j. Update the total number of ions and electrons in each zone after time t

$$Ne[t+1] = Ne[t] + Ce[t] + Ie[t] - Oe[t]$$

where 'Ce[t]' - Change in number of electrons due to ionization or attachment in the zone

'Ie[t]' - Number of electrons drifting in

'Oe[t]' - Number of electrons drifting out

Calculation for positive and negative ions is similar.

k. *Calculate electric field in each zone due to space charge*

Charge density in k-th zone, D[k] = Q*N[t]/S[k]

where 'N[t]' is the resultant number of ions and electrons account for the space charge effect, 'Q' is electron charge 1.602×10^{-19} C, 'S[k]' is the surface area covered by k-th zone.

The change in electric field in k-th zone, $\Delta E[k] = D[k]/\varepsilon$

where 'ε' is the permittivity of free space.

The space charge field in adjacent cells are related by

$$Sp[k] = Sp[k-1] + 0.5(\Delta E[k-1] + \Delta E[k])$$

The field in the first zone is given by $E[1] = Ep + 0.5*\Delta E[1]$

where 'Ep' is the field at the point electrode. The integration of space charge field over all zones should be zero (space charge produces no external voltage on the gap).

i.e. $$\Sigma Sp[k] = 0$$

l. ***Update electric field and hence effective ionization coefficient in each zone***

$$E[t+1,k] = Ebase[k] + Sp[t,k]$$

where 'Ebase[k]' is Laplace electric field.

m. ***Find out the effective ionization coefficient-distance value throughout the gap and proceed to next time step until this value converges***

Normally, using the Pentinum II 233MHz computer, the simulation program execution time for plotting the graph of effective ionization coefficient-distance value (αd) from applied voltage 2 to 100 kV with 1kV step is at least two hour.

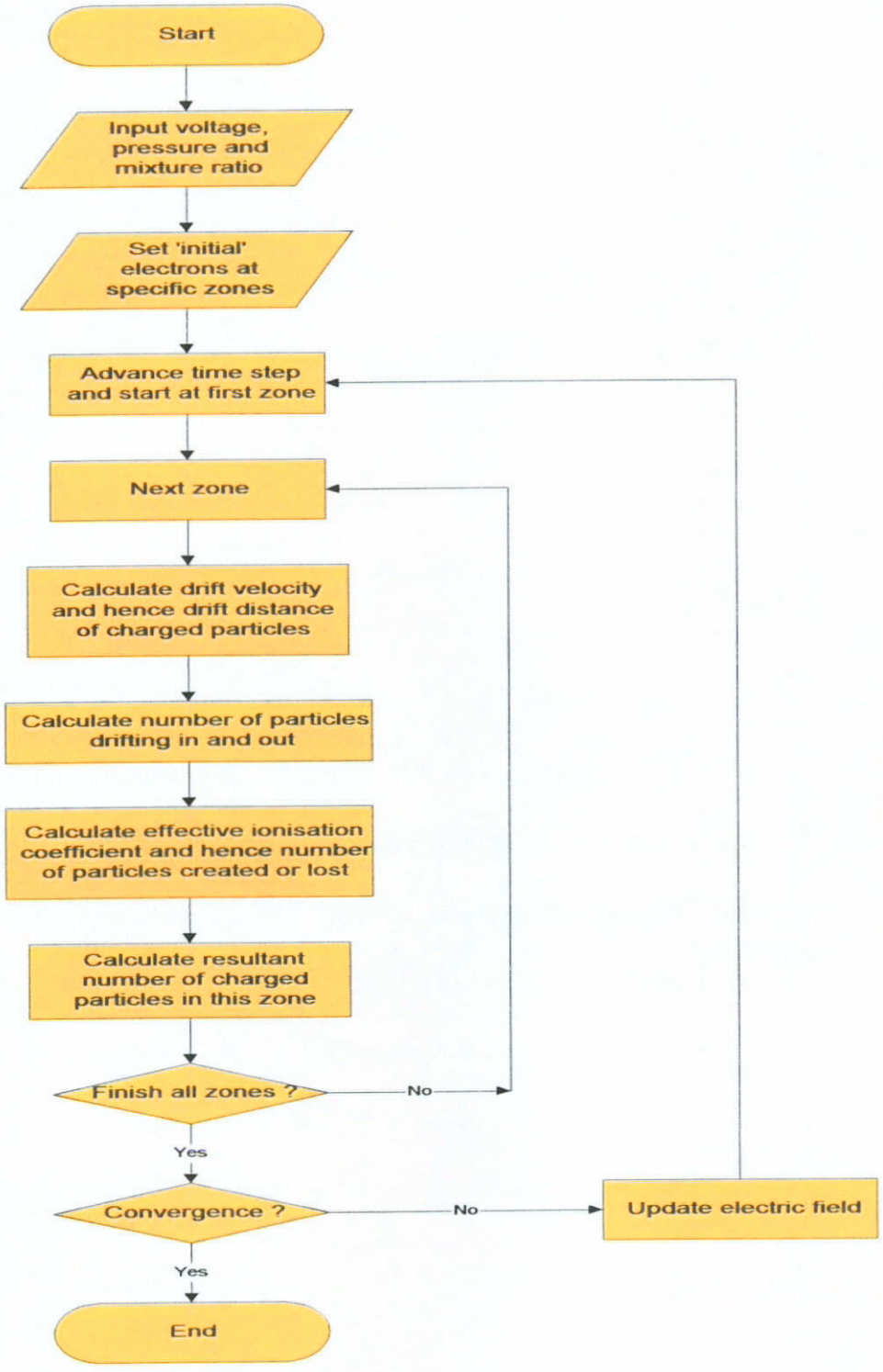

Figure 5.1 : The flowchart of algorithm for space charge simulation for positive corona in steady-state situation

5.3 Simulation result

Using the simulation program of positive corona discharge, we can obtain the result in the following 3 categories:

- Summation of α.dr values at each voltage to determine the K value
- FSOV (Onset or breakdown voltage) under various pressure and SF_6/N_2 mixture content at K=16.1
- SSOV (Breakdown voltage) under various pressure and SF_6/N_2 mixture content as K=16.1

The simulation process is repeated for different voltages, pressures and gas mixture ratios. Figures 5.2, 5.3 and 5.4 show the graphs of K value vs. applied voltage under various pressure and SF_6/N_2 mixture content. In each case, the K value rises quickly to above the critical level (16.1 for pure SF_6 and 18.4 for N_2). This voltage is the first streamer onset voltage (FSOV). Within 5 kV, the K value drops very quickly to very low levels due to the increase in avalanche number and size, which increases the space charge and suppresses the streamers. Then the K value rises gradually until it exceeds the critical level again i.e. the streamers appear again. This is the second streamer onset voltage (SSOV).

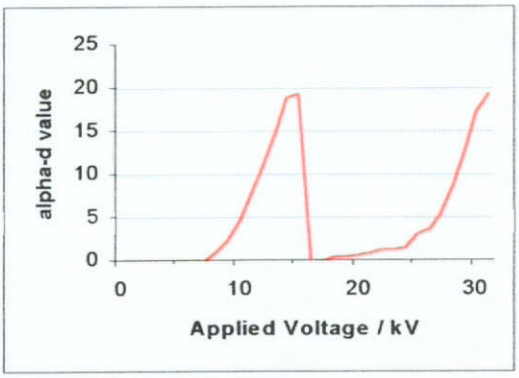

a) 0% SF_6 mixture ratio

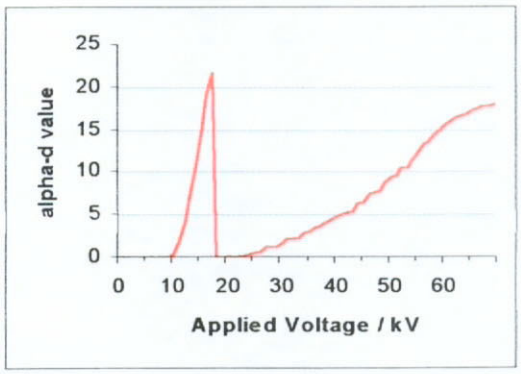

b) 20% SF_6 mixture ratio

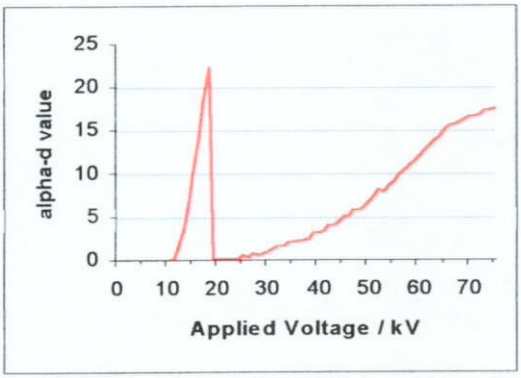

c) 40% SF_6 mixture ratio

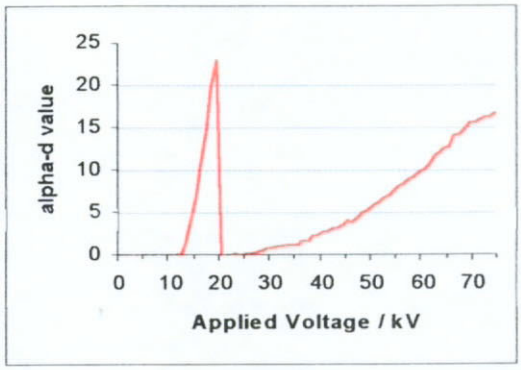

d) 60% SF_6 mixture ratio

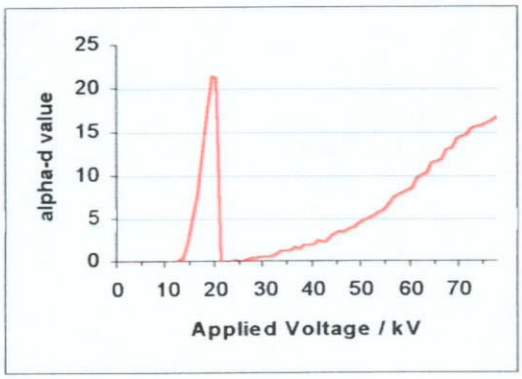

e) 80% SF_6 mixture ratio

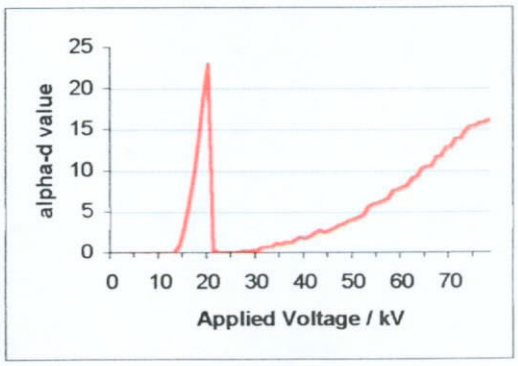

f) 100% SF_6 mixture ratio

Figure 5.2 : The graph of simulated effective ionisation coefficient-distance value vs. applied voltage under various SF_6/N_2 mixture ratio for positive corona in steady-state situation

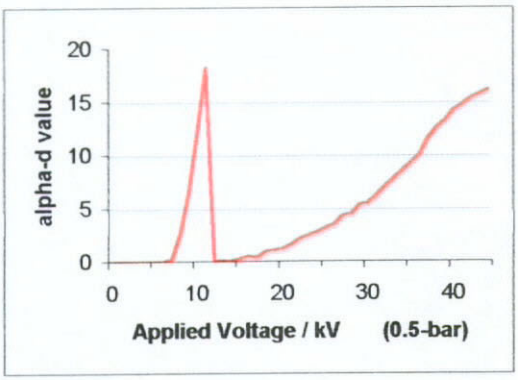

a) 0.5 bar

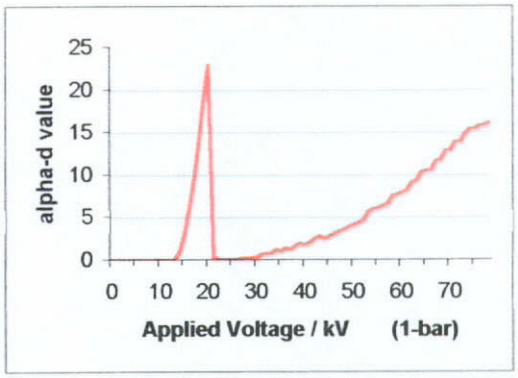

b) 1 bar

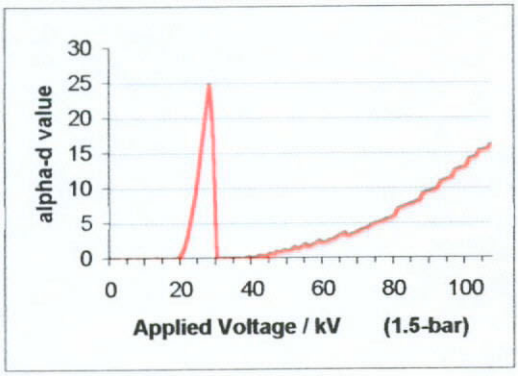

c) 1.5 bar

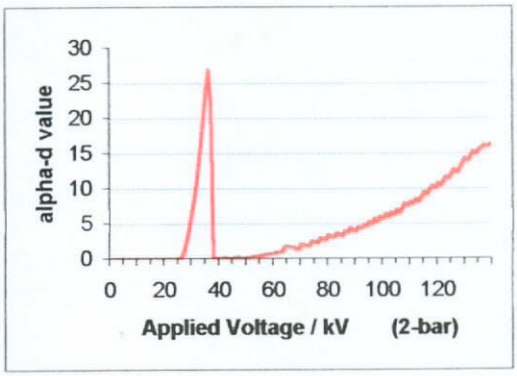

d) 2 bar

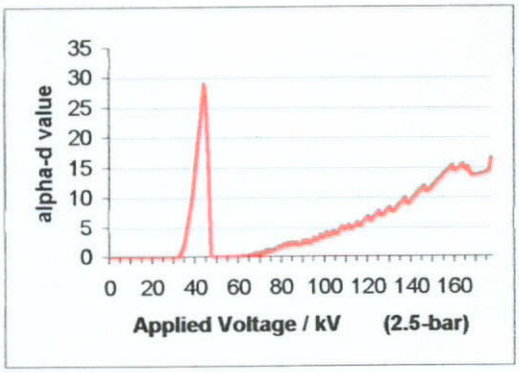

e) 2.5 bar

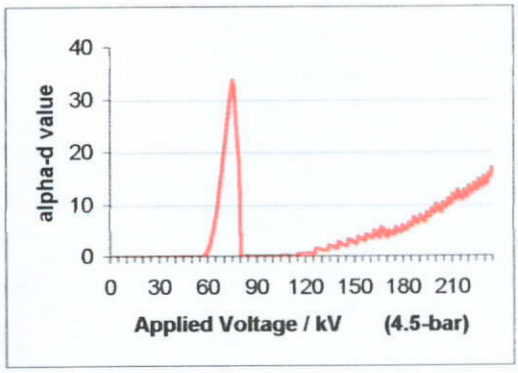

f) 3 bar

Figure 5.3 : The graph of simulated effective ionisation coefficient-distance value vs. applied voltage under various pressure for pure SF_6 for positive corona in steady-state situation

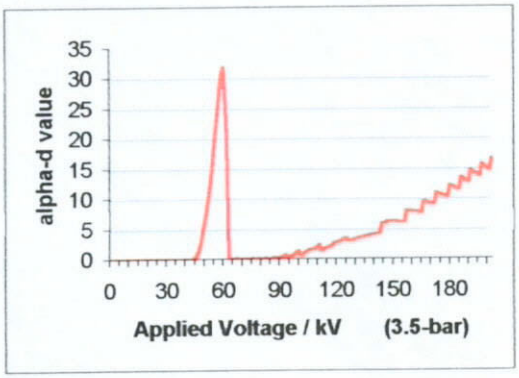

g) 3.5 bar

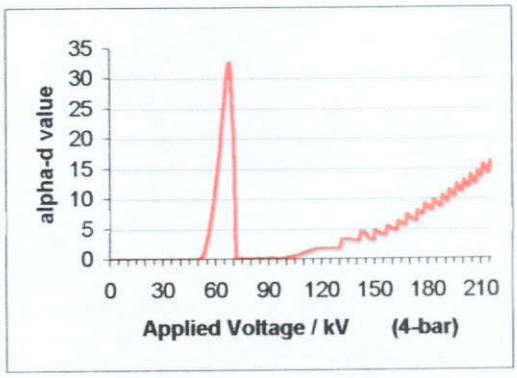

h) 4 bar

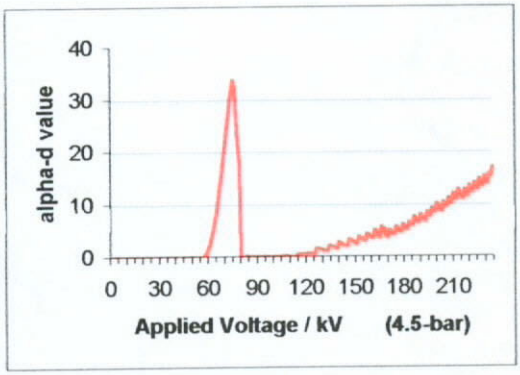

i) 4.5 bar

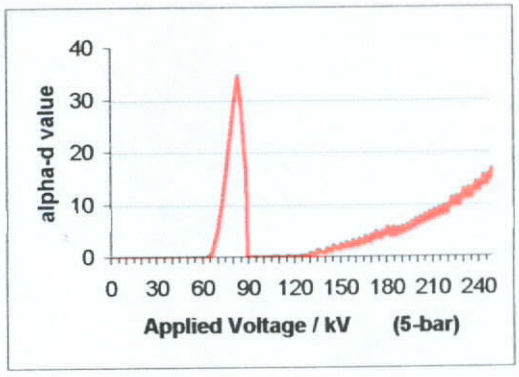

j) 5 bar

Figure 5.3 : The graph of simulated effective ionisation coefficient-distance value vs. applied voltage under various pressure for pure SF_6 for positive corona in steady-state situation (Continued)

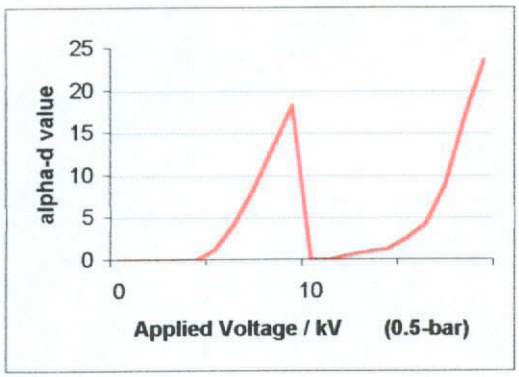

a) 0.5 bar

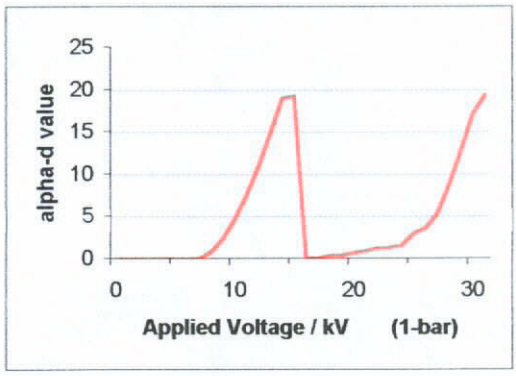

b) 1 bar

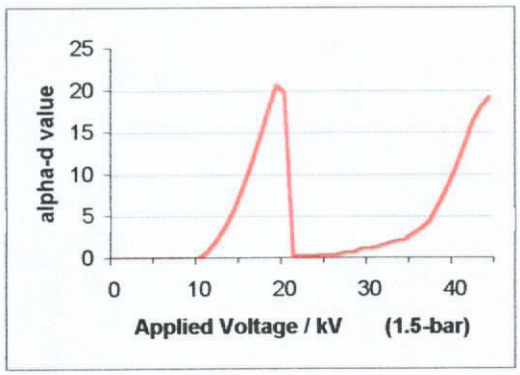

c) 1.5 bar

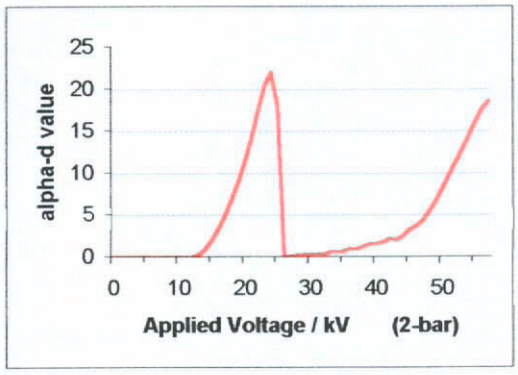

d) 2 bar

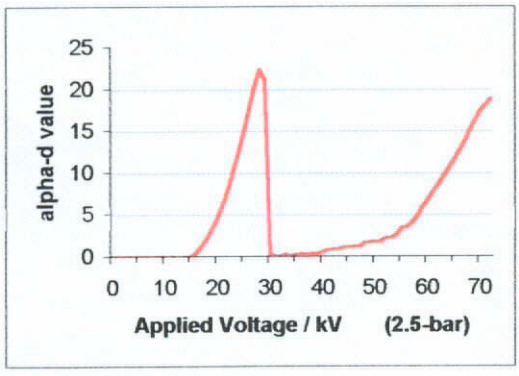

e) 2.5 bar

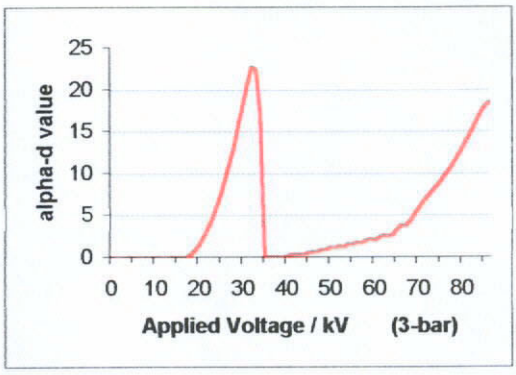

f) 3 bar

Figure 5.4 : The graph of simulated effective ionisation coefficient-distance value vs. applied voltage under various pressure for pure N_2 for positive corona in steady-state situation

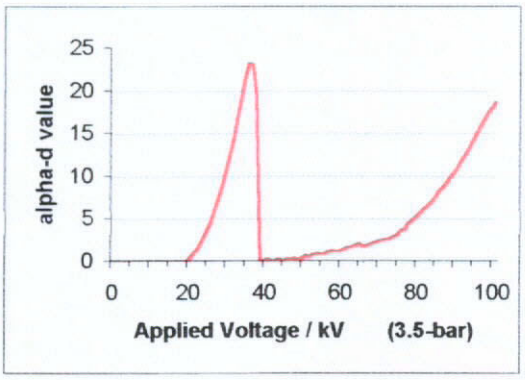

g) 3.5 bar

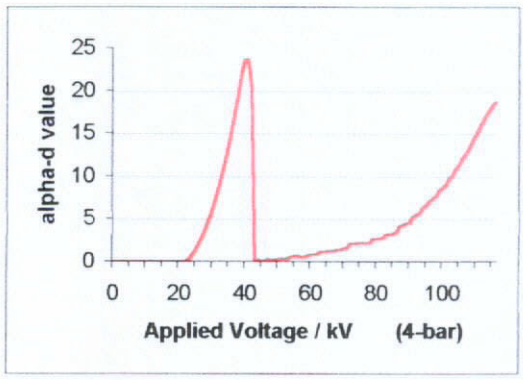

h) 4 bar

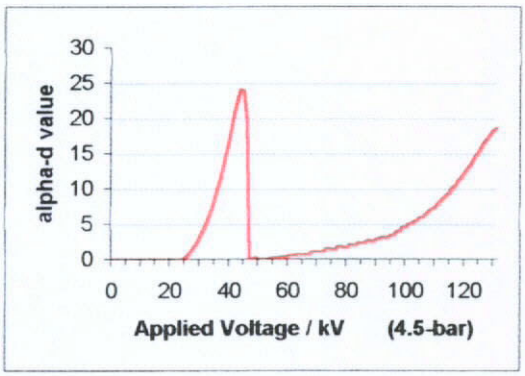

i) 4.5 bar

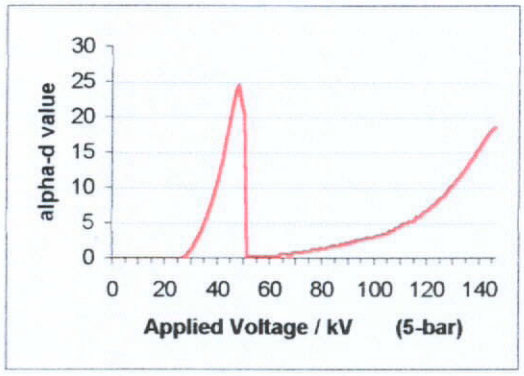

j) 5 bar

Figure 5.4 : The graph of simulated effective ionisation coefficient-distance value vs. applied voltage under various pressure for pure N_2 for positive corona in steady-state situation (Continued)

As the onset voltages are given with reasonable accuracy by the earlier simulation [2] which does not allow for the field-distorting effect of space charge, it may be assumed that, at least up to the onset voltage, space charge has little effect [32]. However, this is no longer the case for relatively small increases above onset voltage. The streamers only occur at the onset voltage and not above. It is clear that space charge, in the form of a 'cloud' of positive ions, must build up around the pointed electrode at, or just above, the onset voltage to the extent that streamers are no longer formed. This is corroborated by the field distributions found by the simulation. A typical graph is shown in Figure 5.5 (which is for 50kV, with SF_6 at 1 bar). The field in the region near the electrode is close to the critical field. Beyond this the field is less than the critical field so no ionisation occurs.

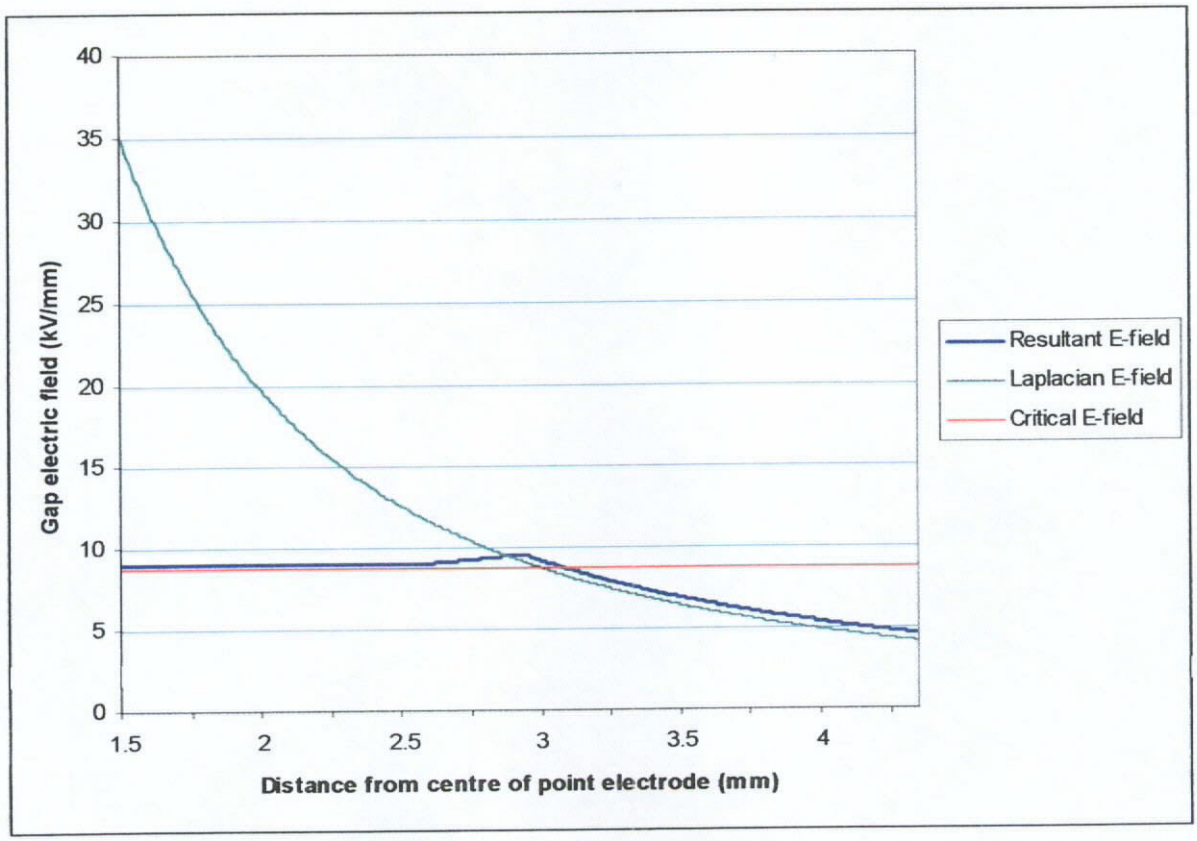

Figure 5.5 : The graph of gap electric fields with distance at 50kV, 3mm diameter point and 1-bar pressure for pure SF_6

There must be a field slightly higher than critical field in the outer space charge region in order to have some avalanches adding positive ions to the region to replace those drifting away. This would be a 'fluctuating equilibrium' rather than a steady equilibrium as although the drift is relatively constant, the avalanches add large quantities of positive ions at particular times and places. This is seen to occur near the outer edge of the space charge region, where the field rises slightly above critical: this small region must supply all the replacement positive ions.

Chapter 6

Discussion

Chapter 6 : Discussion

6.1 Comparison between simulation and experimental results

In Figures 5.3 and 5.4, a reasonable interpretation of the shape of the graphs is that the front of the first peak, at about K=16 (for SF_6) or 18 (for N_2) is the corona onset. While K remains greater than 16, streamers occur, i.e. region (a) in Figure 2.3. The low values of K correspond to the glow region (b) in Figure 2.3 - and as the ionisation increases and K rises towards about 16, streamers again begin to occur, as K increases further, streamers develop into leaders and breakdown occurs. And that this is how the graphs such as those in Figures 5.3 and 5.4 were used to derive the 'simulation' curves in Figures 6.1-6.4.

In Figure 6.1, the graphs of onset voltage and FSOV, and of breakdown voltage and SSOV, show reasonably good agreement. In Figure 6.2, the graph of onset voltage and FSOV against SF_6/N_2 ratio for different pressures shows good agreement between experimental and simulation results.

In Figure 6.3, the graph of FSOV and SSOV from simulation with onset and breakdown voltages from experiment against pressure for 0.5 bar to 5 bars for SF_6 shows that corona onset voltages and breakdown voltages correspond to the FSOV and SSOV respectively for pressure less than 2 bars. The breakdown voltages correspond to the FSOV for pressure larger than 3 bars. And for the intermediate transition region, the onset voltage still corresponds to the FSOV, but the breakdown voltage moves from the SSOV to FSOV.

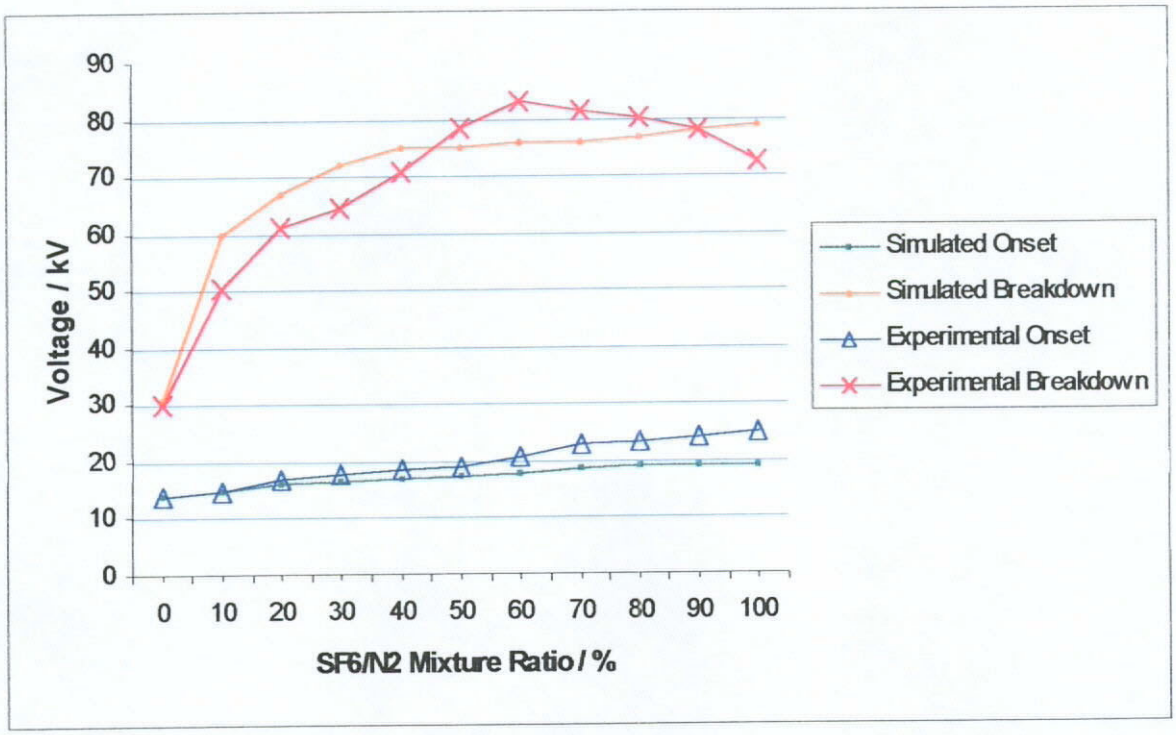

Figure 6.1 : The graph of experimental and simulated onset and breakdown voltages vs. SF_6/N_2 mixture ratio under 1 bar pressure for positive corona in steady-state situation

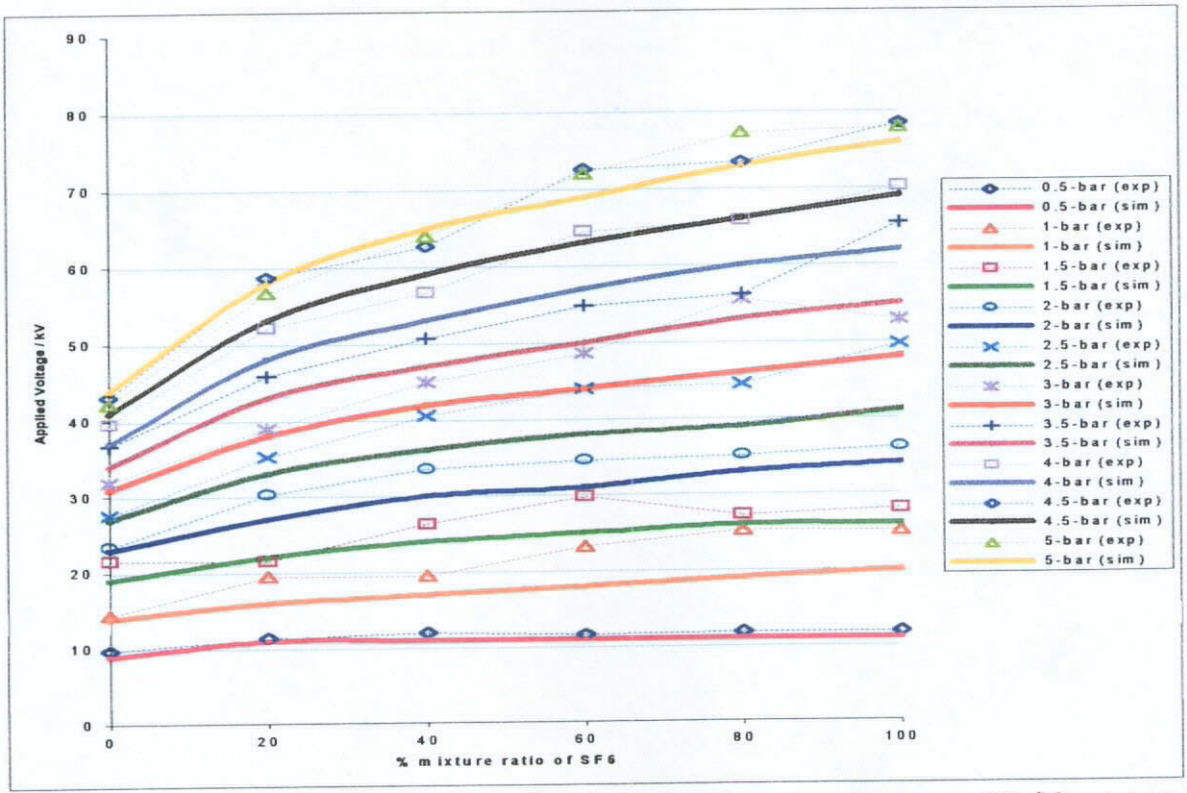

Figure 6.2 : The graph of experimental and simulated onset voltages vs. SF_6/N_2 mixture ratio under various pressure for positive corona in steady-state situation

For the same graph for N_2 in Figure 6.4, the curve profile is similar to SF_6 one but the breakdown voltage and SSOV are much lower than that of SF_6. So it shows that the effective ionisation coefficient is much less for N_2 than SF_6.

The simulation shows that at lower pressures, the breakdown must occur at, or not far above, the simulated SSOV as the K value increases gradually and then exceeds the critical level ('16.1' for pure SF_6) again and continues to increase and hence the size and intensity of the streamers produced continue to increase.

The appearance of experimental intermediate region between the simulated FSOV and SSOV is believed to be due to the steady-state 'continuous ionisation' approach. In practice, positive ions are not produced at a continuous rate, instead avalanches add large amounts of positive ions at particular times and places. So there would be some fluctuations in space charge density due to the significant size of the avalanches. This in turn means that the field there would also fluctuate and occasionally streamers would occur.

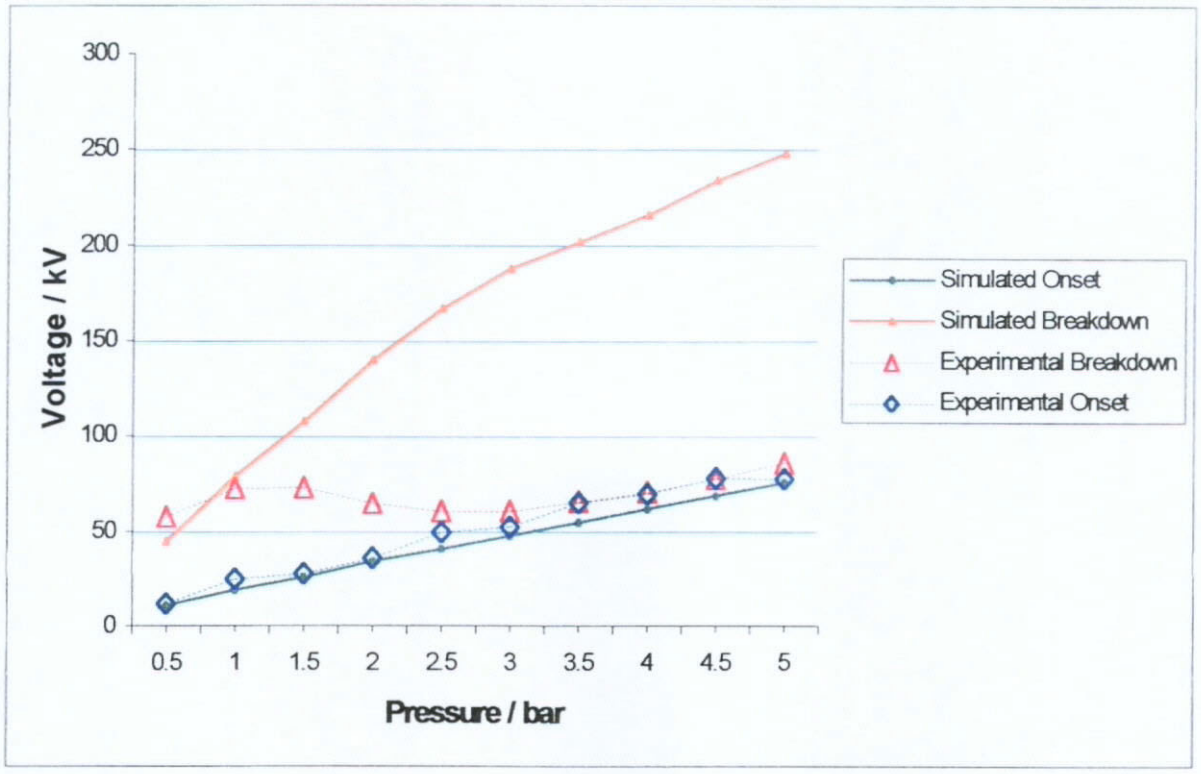

Figure 6.3 : The graph of experimental and simulated onset and voltages vs. pressure for pure SF_6 for positive corona in steady-state situation

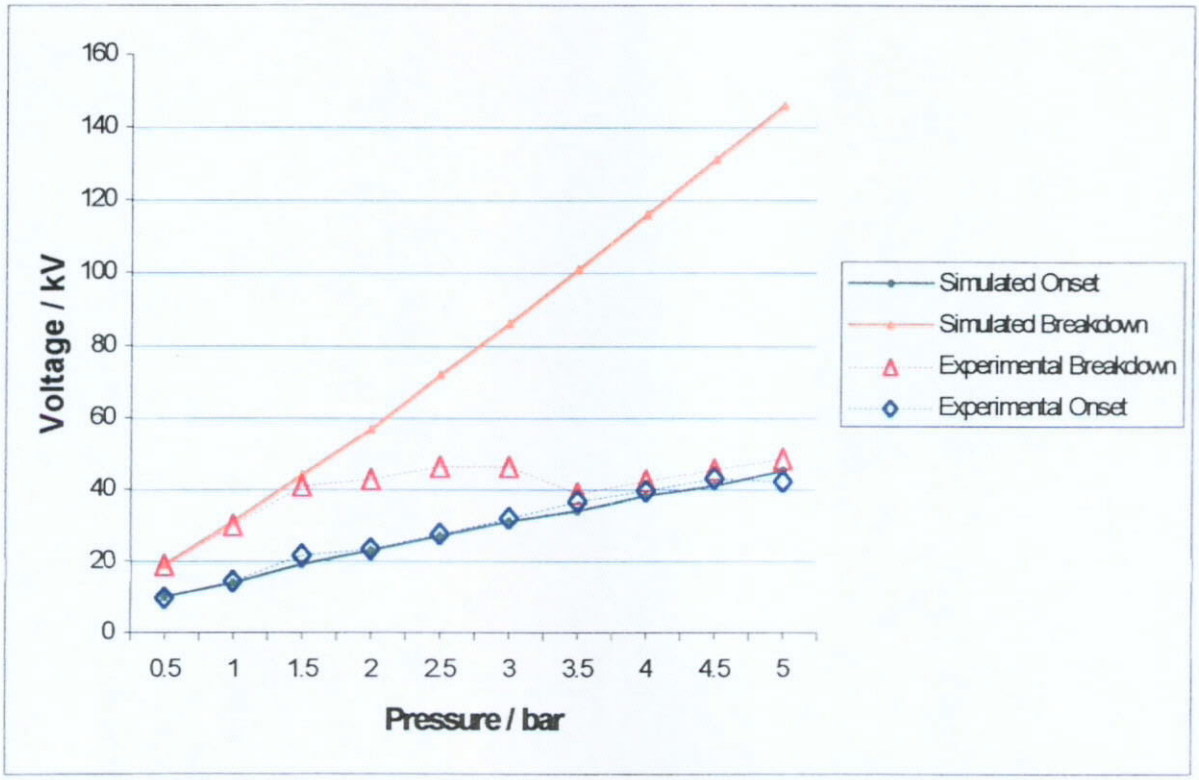

Figure 6.4 : The graph of experimental and simulated onset and voltages vs. pressure for pure N_2 for positive corona in steady-state situation

During the onset, the FSOV is the leading edge of a narrow peak where the K value is around the critical level ('16.1' for pure SF_6) which explains the sudden disappearance of streamers above the onset voltage at lower pressures. The height of the K-peak increases by a factor of two from 0.5 bar to 4 bars (i.e. a large increase in the average size of avalanche). This may be why at the higher pressures (above 3 bars) breakdown occurs at the FSOV rather than the SSOV due to extremely high ionisation rate causing streamer to leader transition. (When K increases from 16.1 to 32, the avalanche sizes increase by a factor of 10^7. When K=32, avalanches would theoretically reach sizes of 10^{14}.)

It appears that the space charge effect becomes less as the pressure increases and at last disappears. So when the pressure is large than 3 bars, the breakdown was observed to occur at once at the onset voltage in the experiment. Then why is the space charge effect reduced? It is clear that the distance travelled by an 'initial' electron in the ionisation region to form an avalanche and become a streamer becomes shorter as the pressure increases. For example, the average distances travelled by the electron to form a streamer at 1, 3 and 5-bar pressures are 40, 20 and 10 μm respectively at the FSOV. Furthermore, at onset voltage, the distance between the critical field boundary and the point electrode surface is longer at lower pressures i.e. bigger volume of the ionisation region. As more positive ions are created in the ionisation region, they accumulate near the point electrode surface more easily. So we believe that the chance of streamer to leader transition is very high under higher pressures as the size of the space charge cloud formed in the ionisation region is smaller. This case is just similar to the parallel plane electrode system in which the

breakdown occurs as the first streamer forms, i.e. at the onset voltage.

Complex simulations including dynamic equilibrium between ion production and drift were developed in order to clarify the space charge densities and dimensions in using SF_6 and N_2 mixture. Although there is some difference between experimental and simulated results of breakdown voltages at the intermediate pressures (1.5 to 2.5 bars), it can simulate the space charge effect generally above the onset voltage and give reasonable estimates of the onset and breakdown voltage values below 1.5 bar and above 2.5 bar.

6.2 Limitations of simulation program

1. The simulation program involves less zones divided and large time step. So they restrict the range of applied voltage and pressure, e.g. if the pressure is set above 5 bars, the overflow problem in the program may occur.

2. The simulation calculates ionisation based on the specific value of ionisation coefficients which are in fact probabilities. So at any voltage, the simulation only indicates a mean size rather than the distribution of sizes of avalanches produced in reality.

3. In the simulation, avalanches are not specifically used and a continuous and non-discrete ionisation is assumed. However, in practice, avalanches occur at random place and time and, as mentioned above, in a range of sizes, so occasionally streamers

will occur even when K<16 in the model. This probably explains how breakdown can occur within the transition region between the FSOV and the SSOV.

6.3 Simple fluctuation simulation

Figures 6.3 and 6.4 show the comparison of experimental and simulated results of onset and breakdown voltages under various pressures. For increased pressures the space-charge region will be correspondingly smaller and the fluctuations about the equilibrium correspondingly greater: this leads towards an explanation of the decreased effectiveness of corona shielding with increased pressure. Figures 6.5-6.8 show how the K value changes with the percentage of electric field fluctuation in ionisation region under different pressure. It can be concluded that at higher pressure, the K value fluctuates significantly and easily rises to critical value just above the onset voltage even a little change of electric field in ionisation region. So for pressure larger than 3 bars, breakdown occurs very close to the onset voltage as explained above.

As the corona discharge simulation is developed to involve dynamic equilibrium between ion production and drift in each divided zone, the local electric field should fluctuate with time. In Figures 6.5-6.8, the graphs of ionisation coefficient-distance value, K under different extent of electric field fluctuation at different pressures are simulated and described. At 3-bar pressure, 17.5% electric field fluctuation will cause K to reach around the critical value after the FSOV and the same effect is found for 15% fluctuation only at 4-bar pressure too. So the fluctuation line indicates the likely explanation of the

'anomalous' breakdown voltage for the intermediate pressure region between 1.5 and 2.5 bars found in the experiments. And the breakdown voltage value increases gradually at 3.5 bars and at higher pressures.

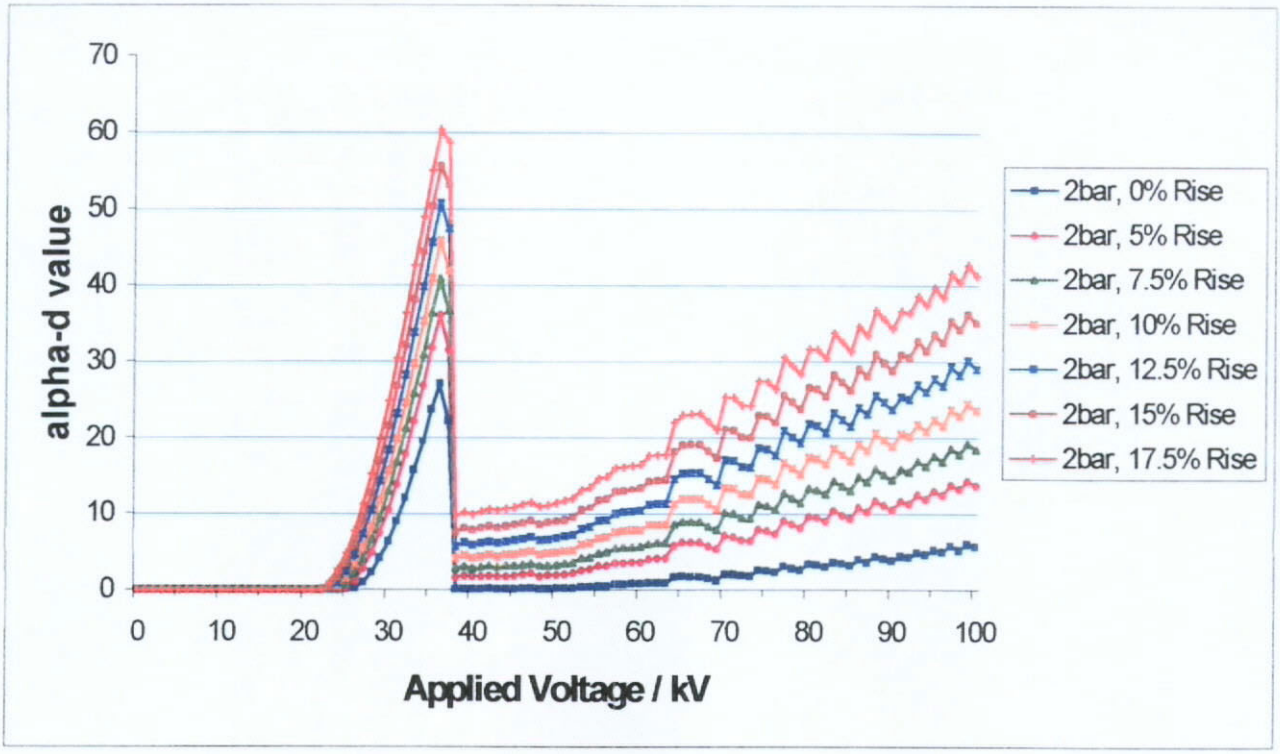

Figure 6.5 : The graph of simulated effective ionisation coefficient-distance value vs. applied voltage under 2 bar pressure for pure SF_6 for positive corona in steady-state situation

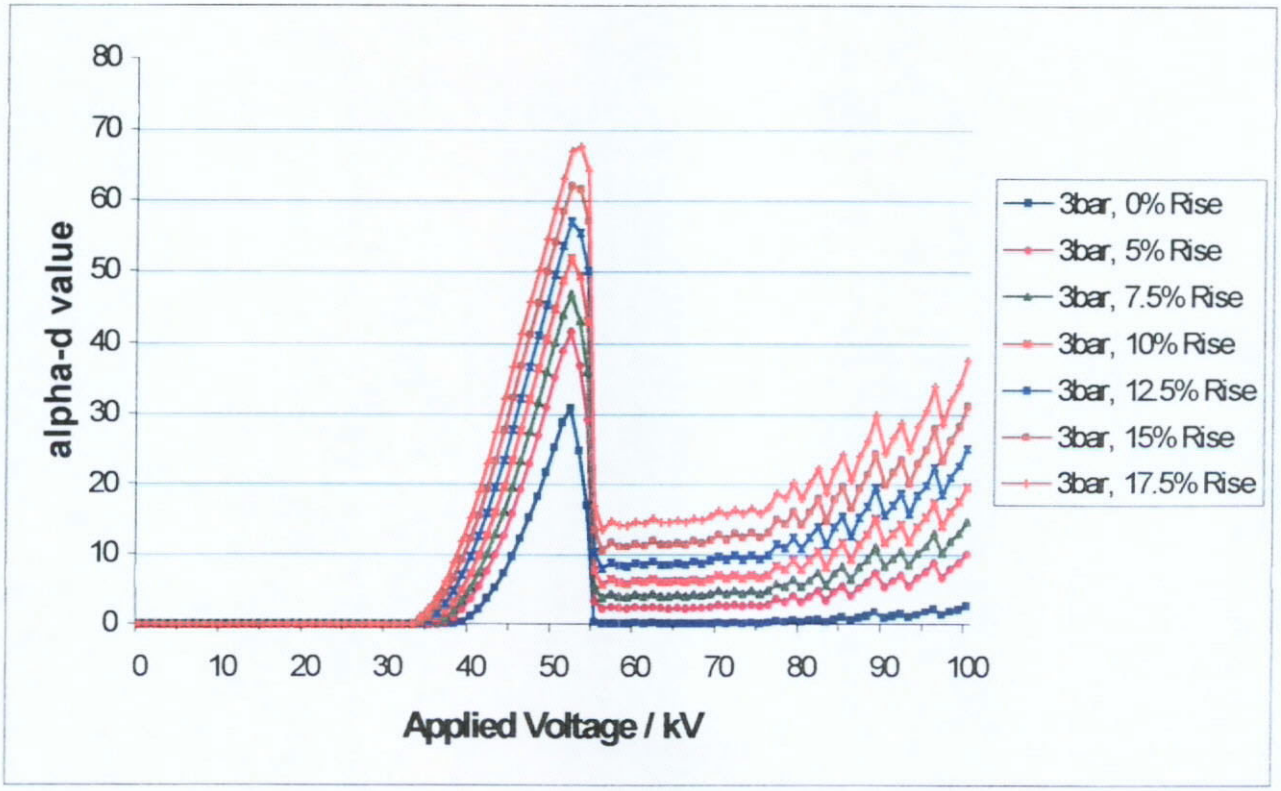

Figure 6.6 : The graph of simulated effective ionisation coefficient-distance value vs. applied voltage under 3 bar pressure for pure SF_6 for positive corona in steady-state situation

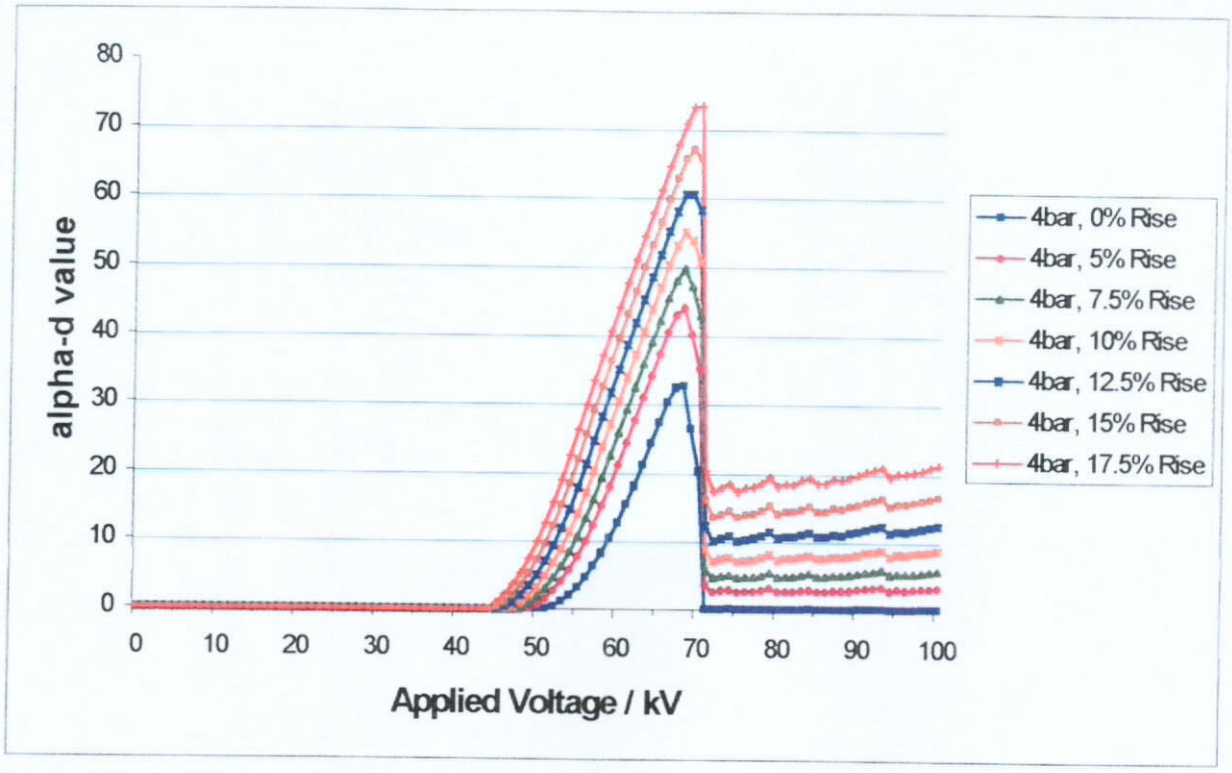

Figure 6.7 : The graph of simulated effective ionisation coefficient-distance value vs. applied voltage under 4 bar pressure for pure SF_6 for positive corona in steady-state situation

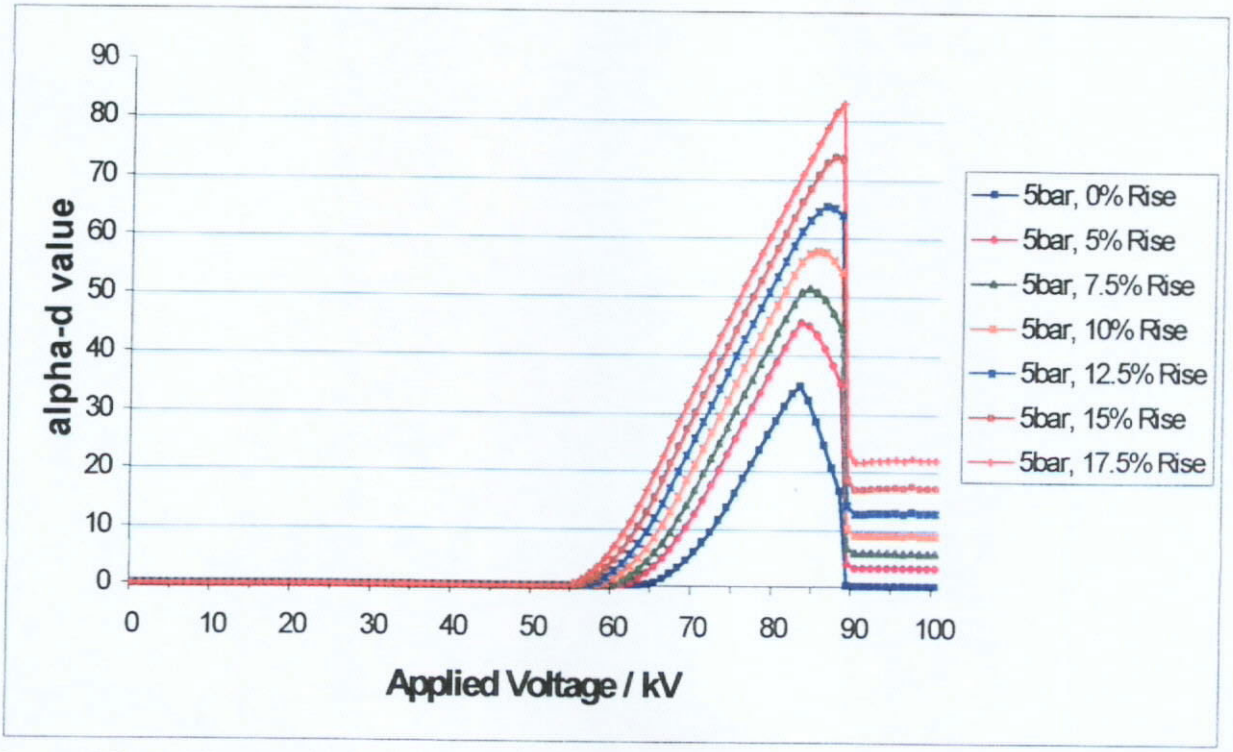

Figure 6.8 : The graph of simulated effective ionisation coefficient-distance value vs. applied voltage under 5 bar pressure for pure SF_6 for positive corona in steady-state situation

Chapter 7

Conclusion

Chapter 7 - Conclusion

1. By using the point/cup electrode geometry, I have successfully simulated the modelling of the space charge near the point electrode for positive-point corona to obtain a dynamic equilibrium between the ionisation, attachment and drift phenomena for SF_6 and N_2 mixtures.

2. The simulation shows that there are two voltages at which streamers start to develop. During the onset, the streamers start to appear. Just above the onset voltage, they decrease and disappear as the positive ion space charge around the point electrode suppresses them. When the applied voltage continues to rise, streamers then occur again and finally the breakdown happens.

3. At lower pressures, the FSOV and SSOV from the simulation agree with the onset and breakdown voltages respectively from the experimental observation. At higher pressures, the FSOV corresponds to the breakdown voltages.

4. For all the mixtures of SF_6 and N_2, there is a good agreement at all pressures considered between the FSOV from the simulation, and the onset voltages from the experimental observation.

5. For all the mixtures of SF_6 and N_2 at low pressures, there is reasonable agreement between the SSOV from the simulation and the breakdown voltage measured.

6. A transition region exists between the low and high pressure regions where the simulated FSOV and experimental onset voltages agree but the breakdown voltages do not. This appears to show the need for a discrete, rather than a continuous, approach to the simulation at this point. This would include the effect of discrete avalanche arrival at the pointed electrode rather than continuous ionisation processes.

References

References

1. N.H. Malik and A. H. Qureshi, "A Review of Electrical Breakdown in Mixtures of SF6 and Other Gases", IEEE Transactions on Electrical Insulation, Vol. EI-14 No.1, February 1979, pp.1-13.

2. Li Er-ning and J.M.K. MacAlpine, "Negative Corona in Air Using a Point/Cup Electrode System", IEEE Transactions on Dielectric and Electrical Insulation, 7, pp.752-757, 2000.

3. S. El-Debeiky, "On The Formation Mechanisms of Positive and Negative Glow Coronas", Proc. IEE, Vol. 123, pp.216-219, 1978.

4. Y. Qiu and Y. P. Feng, "Calculation of Dielectric Strength of the SF_6/N_2 Gas Mixture in Macroscopically and Microscopically Non-Uniform Fields", Proceedings of the 4th International Conference on Properties and Applications of Dielectric Materials, Brisbane Australia, July 3-8, 1994, pp.102-113.

5. N.H. Malik and A.H. Qureshi, "Calculation of Discharge Inception Voltages in SF_6-N_2 Mixtures", IEEE Transactions on Electrical Insulation, Vol. EI-14 No.2, April 1979, pp.70-76.

6. N.H. Malik and A.H. Qureshi, "Breakdown Gradients in SF_6-N_2, SF_6-Air and SF_6-CO_2 Mixtures", IEEE Transactions on Electrical Insulation, Vol. EI-15 No.5, October 1980, pp.413-418.

7. H. Parekh and K.D. Srivastava, "Effect of Avalanche Space Charge Field on the Calculation of Corona Onset Voltage", IEEE Transactions on Electrical Insulation, Vol. EI-14 No.4, August 1979, pp.181-192.

8. L.G. Christophorou and R.J. Van Brunt, "SF_6/N_2 Mixtures – Basic and HV Insulation Properties", IEEE Transactions on Dielectrics and Electrical Insulation, Vol. 2 No.5, October 1995, pp.952-1003.

9. J.M.K. MacAlpine and Yim W. C., "Computer Modelling of Trichel Pulses in Air", Conference on Electrical Insulation & Dielectric Phenomena (CEIPD), 22-25 October 1995, Virginia, USA.

10. O. Farish, O.E. Ibrahim and B.H. Crichton, "Effect of Electrode Surface Roughness on Breakdown in Nitrogen/SF_6 Mixtures", Proc. IEE, Vol. 123, pp. 1047-1050, 1976.

11. J.M.K. MacAlpine, and Shum C.N., "Schottky emission currents in compressed sulphur hexafluoride using a point/cup electrode system", ACED'96, Bangkok,

Thailand, 8th Asian Conference on Electrical Discharges (ACED), 15-17 October 1996, Bangkok, Thailand.

12. M. Ermel, "Electron Emission Currents in Compressed SF_6 in the Coaxial Cylindrical Field", Proc. IEE, Vol. 123, pp. 1047-1050, 1976.

13. J. Charrier, R. Le Ny and A. Boulloud, "Influence of a Spherical Protrusion on One of the Electrodes on the Breakdown Voltage in Room Air", Proc. IEE, Vol. 127, pp. 546-557, 1978.

14. B.H. Crichton, D.I. Lee and D.J. Tedford, "Prebreakdown in Compressed SF_6 and SF_6/N_2 Mixtures in Projection Perturbed Uniform Fields", Proc. IEE, Vol. 129, pp. 134-142, 1979.

15. J. Liu and G.R. Govinda Raju, "Streamer Formation and Monte Carlo Space-charge Calculation in SF_6", IEEE Transactions on Electrical Insulation, Vol. 28, No.2, April 1993, pp.261-270.

16. J.P. Novak and M.F. Frechette, "Transport coefficients of SF_6 and SF_6-N_2 mixtures from revised data", J. Applied Physics, Vol. 55, No.1, 1 January 1984, pp.107-116.

17. S.R. Naidu and K.D. Srivastava, "Volt-Time Curves for a Coaxial Cylindrical Gap in SF_6-N_2 mixtures", IEEE Transactions on Electrical Insulation, Vol. EI-22 No.6, December 1987, pp.755-762.

18. B. Lieberoth-Leden and W. Pfeiffer, "Predischarge Development in N_2 and SF_6 at High Gas Pressure", IEEE Transactions on Electrical Insulation, Vol. 24, No.2, April 1989, pp.285-296.

19. Ziqin Li, R. Kuffel and E. Kuffel, "Volt-Time Characteristics in Air, SF_6/Air Mixture and N_2 for Coaxial Cylinder and Rod-Sphere Gaps", IEEE Transactions on Electrical Insulation, Vol. EI-21 No.2, April 1986, pp.151-155.

20. Jianfen Liu and G.R. Govinda Raju, "Simulation of Corona Discharge - Negative Corona in SF_6", IEEE Transactions on Dielectrics and Electrical Insulation, Vol. 1, No. 3, June 1994, pp.520-529.

21. Jianfen Liu and G.R. Govinda Raju, "Simulation of Corona Discharge - Positive Corona in SF_6", IEEE Transactions on Dielectrics and Electrical Insulation, Vol. 1, No. 3, June 1994, pp.530-539.

22. Y. Shibuya, N. Yamada and T. Nitta, "Electrical Breakdown and Prebreakdown Dark Current in Compressed SF_6".

23. R.J. Van Brunt and M. Misakian, "Mechanisms for Inception of DC and 60-Hz AC Corona in SF6", IEEE Transactions on Electrical Insulation, Vol. EI-17 No.2, April

1982, pp.106-120.

24. G.R. Govinda Raju and M.S. Dincer, "Measurement of ionization and attachment coefficients in SF_6 and SF_6+N_2", J. Applied Physics, December 1982, p.8562.

25. S.El-Debeiky, "On the Formation Mechanisms of Positive and Negative Glow Coronas".

26. R.J. Van Brunt and J.T. Herron, "Fundamental Processes of SF_6 Decomposition and Oxidation in Glow and Corona Discharges", IEEE Transactions on Electrical Insulation, Vol. 25, No.1, February 1990, pp.75-90.

27. M.S. Dincer and T. Aydin, "Simulation of Limiting Field Behavior in Electron Swarms in SF_6/N_2 Gas Mixtures", IEEE Transactions on Dielectrics and Electrical Insulation, Vol. 1, No.1, February 1994, pp.139-145.

28. Li Er-ning and J.M.K. MacAlpine, "Positive Corona in Air Using a Point/Cup Electrode System", Electrical Engineering, The Hong Kong Polytechnic University.

29. F. Pinnekamp and L. Niemeyer, "Qualitative model of breakdown in SF_6 in inhomogeneous gaps", Physics D: Applied Physics, 1983, p.1293.

30. R. Morrow, "Theory of Positive Onset Corona Pulses in SF_6", IEEE Transactions on Electrical Insulation, Vol. 26, No.3, June 1991, pp.398-403.

31. A.H. Mufti, A.A. Arafa and N.H. Malik, "Corona Characteristics for Free Conducting Particles in Various SF_6-Gas Mixtures", IEEE Transactions on Electrical Insulation, Vol. 1, No.3, June 1994, pp.509-516.

32. R. Hazel and E. Kuffel, "Static Field Anode Corona Characteristics in Sulphur Hexafluoride", IEEE Transactions on Power Apparatus and Systems, Vol. PAS-95, No.1, February 1976, pp.178-186.

33. J.K. Nelson, "Positive Corona Processes in Electronegative Gaseous Dielectrics", IEEE Transactions on Electrical Insulation, Vol. EI-20, No.3, June 1985, pp.601-607.

34. Jianfen Liu and G.R. Govinda Raju, "The Nonequilibrium Behavior of Electron Swarms in Nonuniform Fields in SF_6", IEEE Transactions on Plasma Science", Vol. 20, No.5, October 1992, pp.515-523.

35. G.R. Govinda Raju and J. Liu, "Simulation of Electrical Discharges in Gases – Uniform Electric Fields", IEEE Transactions on Dielectrics and Electrical Insulation, Vol. 2, No.5, October 1995, pp.1004-1012.

36. R. Hazel and E. Kuffel, "Static Field Anode Corona Characteristics in Sulphur

Hexafluoride", IEEE Transactions on Power Apparatus and Systems, Vol. PAS-95, no.1, January 1976, pp.178-186.

37. R.J. Van Brunt and D. Leep, "Characterization of Point-Plane Corona Pulses in SF_6", J. Applied Physics 52(11), November 1981, pp.6588-6560.

38. T. Nitta and Y. Shibuya, "Electrical Breakdown of Long Gaps in Sulphur Hexafluoride", Proc. Phys. Soc., Vol. 87, pp.1065-1071, 1978.

39. R. Morrow, "A Survey of the Electron and Ion Transport Properties of SF_6", IEEE Transactions on Plasma Science, Vol. PS-14, No.3, June 1986.

40. N.H. Malik, A.H. Qureshi and Y.A. Safar, "DC Voltage Breakdown of SF_6-Air and SF_6-CO_2 Mixtures in Rod-Plane Gaps", IEEE Transactions on Electrical Insulation, Vol. EI-18, No.6, December 1983, pp.629-635.

41. R.M. Banford, "Particles and Breakdown in SF_6 – Insulated Apparatus", Proceedings of IEE, Vol. 123, No.9, September 1976, pp.877-881.

42. R.E. Wootton, "Some Aspects of Breakdown in Gases", IEEE Transactions on Electrical Insulation, Vol. EI-17, No.6, December 1982, pp.499-504.

43. P.R. Howard, "Processes Contributing to the Breakdown of Electronegative Gases in Uniform and Non-uniform Electric Fields", Proceedings of IEE, Vol. 123, No.9, September 1976, pp.634-639.

44. P.R. Howard, "Insulation Properties of Compressed Electronegative Gases", Proceedings of IEE, Vol. 125, No.9, June 1978, pp.125-130.

45. T.R. Foord, "Some Experiments of Positive Point-to-Plane Corona and Spark Breakdown of Compressed Gases", Proceedings of IEE, Vol. 100, No.78, December 1953, pp.585-591.

46. S.K. Dhali and A.K. Pal, "Numerical Simulation of Streamers in SF_6", J. Applied Physics 63(5), March 1988, pp.1355-1358.

47. X. Xu and S. Jayaram, "Prediction of Breakdown in SF_6 under Impulse Conditions", IEEE Transactions on Dielectrics and Electrical Insulation, Vol. 3 No.6, December 1996, pp.836-842.

48. H. Parekh and K.D. Srivastava, "Some Computations and Observations on Corona-Stabilized Breakdown in SF_6", IEEE Transactions on Electrical Insulation, Vol. EI-15, No.2, April 1980, pp.87-94.